AN EXPERIMENTAL TECHNIQUE FOR DYNAMIC ANALYSIS OF FLEXIBLE DISK DRIVE READ/WRITE HEAD DESIGNS

By

DENNIS LYNN MILLER

Bachelor of Science in Mechanical Engineering

Oklahoma State University

Stillwater, Oklahoma

1984

Submitted to the Faculty of the Graduate College
of the Oklahoma State University
in partial fulfillment of the requirements
for the Degree of
MASTER OF SCIENCE
December, 1985

AN EXPERIMENTAL TECHNIQUE FOR DYNAMIC

ANALYSIS OF FLEXIBLE DISK DRIVE

READ/WRITE HEAD DESIGNS

Thesis Approved:

J. K. Good

Thesis Adviser

R W Worrell

R L Lowery

Norman N. Durham

Dean of the Graduate College

ACKNOWLEDGMENTS

I would like to express my sincere appreciation to all of those who have assisted me during the course of this study. Special words of appreciation go to Dr. J. K. Good, my thesis adviser, for his encouragement, guidance, and never ending patience throughout my graduate studies. I would also like to thank my other committee members, Dr. R. L. Lowery and Dr. P. M. Moretti, for their advisement and participation in the review of this study.

I owe special thanks to my parents, who have not only provided financial assistance but also loving encouragement throughout. I would also like to thank my sister Melinda, and my brother Randy, for their continuous encouragement and refreshing outlooks.

Final words of appreciation are directed to Ms. Charlene Fries for her assistance in the preparation of the final manuscript.

TABLE OF CONTENTS

Chapter		Page
I.	INTRODUCTION	1
	Overview	1
	Literature Survey	4
	Statement of Problem	6
	Approach to the Problem	7
	Organization	7
II.	DEVELOPMENT OF REFLECTED BEAM ANALYZER SYSTEMS	8
	Advantages and Disadvantages of the RBA Systems	11
	L-RBA System Equations	12
	A-RBA System Equations	17
	Calibration of L-RBA System	23
	Calibration of A-RBA System	37
III.	EXPERIMENTAL PROCEDURE	50
	Production Head and Experimental Head Designs	50
	Analyses Using the L-RBA System	51
	Analyses Using the A-RBA System	55
IV.	EXPERIMENTAL RESULTS	60
	Results Using the L-RBA System	61
	Results Using the A-RBA System	78
V.	CONCLUSIONS	99
	Conclusions Regarding Head/Disk Interaction and Stylus Motion	99
	Conclusions Regarding RBA System Accuracy and Resolution	102
	Recommended RBA System Refinements	103
REFERENCES		105
APPENDIX		107

LIST OF TABLES

Table		Page
I.	Output Voltages and Sensitivities Obtained From Static Calibration of the Linear Lateral-Effect Photodiode	26
II.	Peak-to-Peak Output Voltages From L-RBA System Calibration for a Peak-to-Peak Rotation Amplitude of 0.00127 Radians	31
III.	Output Voltages From L-RBA System Calibration Using Vertical Translation	35
IV.	Output Voltages (in Volts) From X-Axis of Array Detector One for Beam Positioned at a Point (X,Y) on the Detector Face	41
V.	Output Voltages (in Volts) From Y-Axis of Array Detector One for Beam Positioned at a Point (X,Y) on the Detector Face	42
VI.	Output Voltages (in Volts) From X-Axis of Array Detector Two for Beam Positioned at a Point (X,Y) on the Detector Face	43
VII.	Output Voltages (in Volts) From Y-Axis of Array Detector Two for Beam Poistioned at a Point (X,Y) on the Detector Face	44
VIII.	Average Output Voltage From Detector One for a Given Beam Position in the X- and Y-Directions	47
IX.	Average Output Voltage From Detector Two for a Given Beam Position in the X- and Y-Directions	47
X.	Dominant High-Frequency Pitch Mode of the Production Head at 300 RPM Drive Speed in the Outside, Middle, and Inside Radial Track Positions	65

Table

Page

XI. Dominant High-Frequency Roll Mode of the Production Head at 300 RPM Drive Speed in the Outside, Middle, and Inside Radial Track Positions 65

XII. Amplitude of 3550 Hz Pitch Mode of the Production Head for Various Media Velocities 67

XIII. Amplitude of Dominant High-Frequency Pitch Modes of AD-2 for Outside and Inside Radial Track Positions and Various Drive Speeds 70

XIV. Amplitude of Dominant High-Frequency Roll Modes of AD-2 for Outside and Inside Radial Track Positions and Various Drive Speeds 71

XV. Amplitude of Dominant High-Frequency Pitch Modes of AD-3 for Outside and Inside Radial Track Positions and Various Drive Speeds 75

XVI. Amplitude of Two High-Frequency Roll Modes of AD-3 for Outside and Inside Radial Track Positions and Drive Speeds of 300 and 240 RPM 76

XVII. Amplitude of 1825 Hz Roll Mode of AD-4 for Outside and Inside Radial Track Positions and Various Drive Speeds 79

XVIII. Displacement Amplitudes of the Production Head in Steady-State Operation 83

XIX. Maximum Displacement Amplitudes of the Production Head 83

XX. Steady-State Offset and Maximum Rotation Amplitudes of the Production Head and AD-4 91

LIST OF FIGURES

Figure		Page
1.	Typical Two-Head System	2
2.	Schematic of Reflected Beam Analyzer	9
3.	Stylus With Mirror Attached to Ferrite Core	10
4.	Definition of Degrees of Freedom Associated With Read/Write Head Displacements	10
5.	Reflected Beam Displacement Due to Vertical Translation	13
6.	Reflected Beam Displacement Due to Rotation	15
7.	A-RBA System	18
8.	Reflected Beam $\vec{R}$ in the Y-Z Plane	19
9.	UDT LSC-5D Lateral-Effect Photodiode	24
10.	Output Voltage Versus Beam Position for Linear Lateral-Effect Photodiode	27
11.	Mechanism Used to Calibrate L-RBA System Using Pure Rotation	29
12.	Output Voltage Versus Excitation Frequency for the L-RBA System Subjected to a Mirror Rotation of 0.00127 Radians	32
13.	Mechanism Used to Calibrate L-RBA System Using Vertical Translation	33
14.	Output Voltage Versus Translation Amplitude for the L-RBA System Set at Various Incident Angles	36
15.	UDT PIN-SC/10D Two-Axis Lateral-Effect Photodiode	38
16.	Output Voltage Versus Beam Displacement Along the Null X-Axis of Array Photodiode	45

Figure Page

17. Output Voltage Versus Beam Displacement Along the Null Y-Axis of Array Photodiode 46

18. Average Output Voltage Versus Beam Displacement in X-Direction for Central 25 Percent Portion of Array Photodiode 49

19. Gimbal System and Stylus of a Production Read/Write Head 52

20. Experimental Design AD-2, Graphite-Epoxy Ring Adhered to Gimbal Structure 52

21. Experimental Design AD-4, LD-400 Damping Material Adhered to Gimbal Structure 53

22. Disk Drive Positioned in the L-RBA System 53

23. Disk Drive Positioned in the A-RBA System 56

24. Schematic of A-RBA System Instrumentation 58

25. Pitch and Roll Spectra of Two Production Heads 62

26. Pitch and Roll Spectra for Production Head, Drive Speed 300 RPM, Outside Radial Track 64

27. Pitch Rotation Amplitude Versus Media Velocity, 3550 Hz Pitch Mode, Outside Radial Track 68

28. Pitch and Roll Spectra for AD-2, Drive Speed 300 RPM, Outside Radial Track 72

29. Pitch and Roll Spectra for AD-3, Drive Speed 300 RPM, Outside Radial Track 74

30. Pitch and Roll Spectra for AD-4, Drive Speed 300 RPM, Outside Radial Track 77

31. Steady-State Response of Production Head, Signals Due to Pitch Rotation and Vertical Translation 81

32. Steady-State Response of Production Head, Signals Due to Roll Rotation 82

33. Production Head Response at Startup, Pitch Signal 87

34. Production Head Response at Startup, Roll Signal 88

Figure

Page

35. AD-4 Response at Startup, Pitch Signal 89

36. AD-4 Response at Startup, Roll Signal 90

37. Stationary Wavefront Formed Upstream of Slider 93

38. Production Head Response After Drive Shutoff 94

39. AD-4 Response After Drive Shutoff 95

40. Spectra Representing Correlation Between Pitch and Roll Modes of the Production Head 97

CHAPTER I

INTRODUCTION

Overview

The flexible disk drive is a popular device which is used to store and retrieve digital information. The first flexible or "floppy" disk system, produced in 1971 by the IBM Corporation [1], made use of an 8-inch flexible disk and was a read-only device. Today, there are many popular flexible disk systems which are built by a multitude of manufacturers.

In the most general form, a flexible disk drive consists of a device to rotate the flexible disk and a read/write head which is used to transfer data to and from the disk. The surface of the flexible disk is coated with a magnetic substrate which allows for storage of digital data in binary form. Since binary numbers can be represented as a zero or one, the digital data can be stored on the disk surface as magnetic flux reversals of either North-South or South-North polarity. Flexible disk systems have evolved from the original 8-inch read-only systems to very sophisticated $5\frac{1}{4}$- and $3\frac{1}{2}$-inch systems which have the capability to both read and write. There are numerous differences in the pioneering systems and those available today.

Probably the most important component of a flexible disk drive is the read/write head. Most flexible disk systems currently in production have two read/write heads--one for each side of the disk. Figure 1

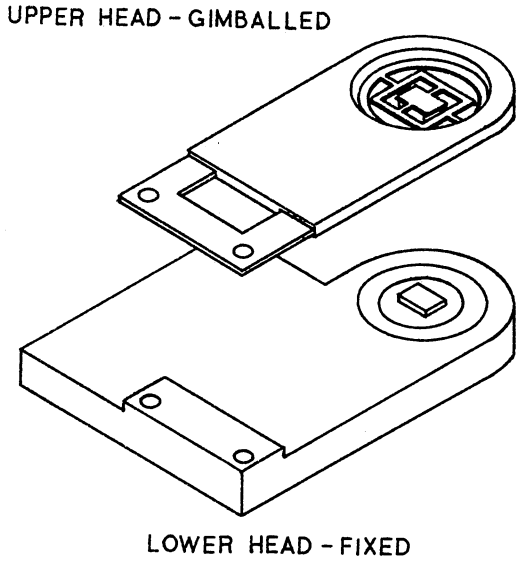

Figure 1. Typical Two-Head System

depicts one such two-head system design. Often the term read/write head will be used synonymously with the term slider. The slider is actually the portion of the read/write head which comes into contact with the flexible disk surface. The flexible disk is positioned between the upper and lower head. Note that the lower slider is rigidly fixed to its positioning arm while the upper slider is affixed to its positioning arm by means of a flexible gimbal structure. The gimbal structure is stamped or etched from a thin metal sheet and provides flexibility in two rotational directions as well as flexibility for vertical translation. The gimbal system was a necessary development to assure proper compliance between the slider and disk. Previous designs which used rigidly fixed sliders in both upper and lower heads did not provide sufficient head/disk compliance, resulting in excessive head bounce and media wear; however, the gimballed systems are not without their own problems. The flexibility of the gimbal structure provides lower head system stiffness and thus allows for vibrational modes which are thought to increase wear of the media and stylus.

As increases in storage capacity and data transfer rates are required, these vibrations could also lead to data errors caused by signal loss and excessive bit shift. Signal loss occurs when the separation between the stylus and disk surface is too large to read or write data. Bit shift is the variation between where a data bit is expected to be and where it actually is. An understanding of the vibration caused by head/disk interface will provide valuable information concerning future read/write head designs.

Literature Survey

Studies of Flexible Disk Systems

There have been many studies conducted to examine the effects of head disk interface in flexible disk systems. The literature search failed to locate a great number of studies which examine the vibration of the head system, as most of these studies are concerned with the head/disk compliance and separation between the slider and disk.

Engh [1] discusses the early development of flexible disk systems. Of particular interest is his discussion of factors such as disk velocity, disk surface lubrication, head/disk compliance, head design, media wear, and the effects of these items on attempts to increase disk capacity.

Greenberg [2] performed an analytical examination of the effects of head/disk interface. The study examines disk response due to interaction with the read/write head. The study makes use of the steady-state Reynolds equation in determining head flying height. The analytic flying height was compared to the experimental data obtained by Charbonnier [3].

Smith and Ragle [4] used white light interferometry to examine head/disk separation in a high speed flexible disk system. A point of interest in this study is the examination of the effects of longitudinal slots in the face of the slider.

Lin [5] suggests three possible techniques for use in the measurement of head/disk separation. The paper cites use of capacitive and inductive systems as well as optical interference methods. Capacitive and inductive methods have the advantage of having sufficient frequency response; however, necessary calibration and the need for head alteration

and a metallic disk surface makes use of these techniques difficult and questionable in regard to validity. Optical interference methods have the advantage of high resolution but an examination of frequency content is near impossible.

Chiou [6] examines the effect of spring pad loading and head penetration on the flying height of a flexible disk over a spherical head. The study presented uses stroboscopic white light interferometry. Reference is made to previous experimental studies which used similar methods with differing disk system parameters.

Good [7], Vickery et al. [8], and Swedeen [9] have examined the low-frequency vibration of an 8-inch flexible disk system. The analyses were conducted using an optical lever technique to examine rotation and vertical translation of the read/write head. These studies considered the effects of media velocity and differing media types.

Bouchard et al. [10] present an interesting analysis of $5\frac{1}{4}$- and 8-inch Winchester-type drives. Their study utilizes a laser Doppler vibrometer to examine the frequency response of the read/write heads (slider and suspension system) as well as the rigid disk itself. The laser Doppler vibrometer measures the frequency shift of laser light reflected from a moving surface. The frequency shift is proportional to the velocity of the motion component which is parallel to the laser beam; thus the use of this system is limited to examination of vertical motions only. Displacements can be calculated from the velocity data but the absolute position is unobtainable.

Experimental Systems for Measuring Small Vibrations

Since few studies were found to consider the vibration of read/

write heads, a search was conducted to locate several means by which head vibrations could be determined experimentally.

Pinder and Palmer [11] discuss an optical level technique which is noninterferometric and does not require a coherent light source. This system has been used to monitor vibrations of at least 5 KHz. Cook and Hamm [12] examine the use of a noncontacting fiber optic lever system.

Ueha et al. [13] present the use of an optical heterodyne technique for vibration measurement. Garza and Sharp [14] describe the use of holographic interferometry for precise analysis of structural systems. An item of special interest presented in this paper is the modal analysis performed on a rigid disk head flexure. Kelly [15] discusses the use of a lateral effect photodiode system for measuring angular rotation of a mirrored surface.

Statement of Problem

This study will be an attempt to experimentally determine the effects of head/disk interaction in a flexible disk system. Of particular interest is the high-frequency vibration of the gimballed upper head system of the drive under investigation. For the purpose of this study, high frequency will refer to those frequencies of 1000 Hz and above. These high frequency vibrations are thought to be possible causes of signal loss and excessive wearing of the stylus and disk media. A portion of this study will be dedicated to examination of the low-frequency motion that occurs as a result of the interaction of the head system with the flexible disk. An instrumentation system capable of accurately determining the head motions associated with head/disk interaction is a necessity in the analysis of new and existing head system designs.

Approach to the Problem

This study will utilize two similar instrumentation systems that were developed to investigate the motion of the read/write head. The analyses will be performed in both the frequency and time domain. The studies in the frequency domain will utilize a Fast Fourier Transform (FFT) algorithm to determine the amplitude and frequency of active vibrational modes. The studies in the time domain will examine head position as a function of time and maximum displacement amplitudes as well as the steady-state operating position of the stylus. The transient response of the read/write head will be examined for both startup and shutdown of the disk drive. Less intensive studies are to be performed to examine the effects that disk media velocity and radial track position have on the amplitude of stylus motion.

Organization

Chapter II will discuss the theory of operation and calibration procedure of the instrumentation systems that are utilized in this study. Chapter III describes the procedures and equipment that are used in the experimental analysis. Chapter IV presents the results of the experimentation. Conclusions and an appraisal of the results are given in Chapter V.

CHAPTER II

DEVELOPMENT OF REFLECTED BEAM ANALYZER SYSTEMS

The instrumentation systems that are to be used in this study make use of an optical lever technique to measure the vibration of the read/write head. A simple schematic of such a system is depicted in Figure 2. These systems will be called Reflected Beam Analyzers and in reference the acronym RBA will be used. In the RBA systems, a laser beam is reflected from a tiny mirror mounted rigidly to a ferrite core which extends from the stylus as shown in Figure 3. The reflected laser beam is displaced when movement of the stylus occurs. A lateral-effect photodiode is used to measure the displacement of the reflected laser beam. Analysis of the movement of the reflected beam will yield the movement of the head system.

Before proceeding with the discussion of the RBA systems, it is necessary to define the degrees of freedom associated with motion of the read/write head. A fairly standard convention is represented in Figure 4. A rotation about the x-axis of the stylus will be designated as a pitch rotation and, likewise, rotations about the y-axis and z-axis will be referred to as roll and yaw, respectively. A translation in the z-direction will be denoted as vertical translation. Other degrees of freedom are neglected as the gimbal structure effectively restrains them.

Two different RBA systems were developed for use in this investigation. The first system is a single output system which utilizes a linear

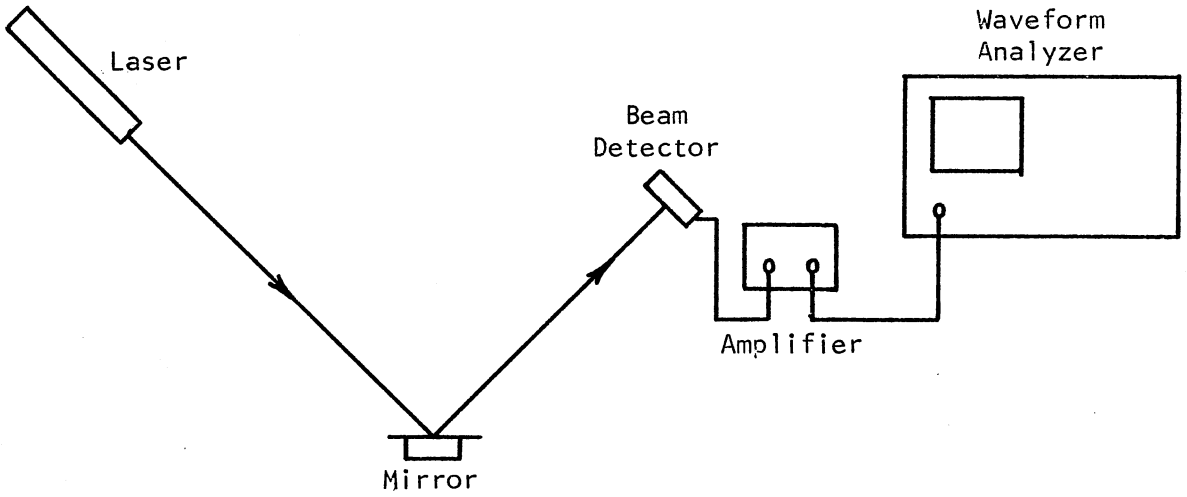

Figure 2. Schematic of Reflected Beam Analyzer

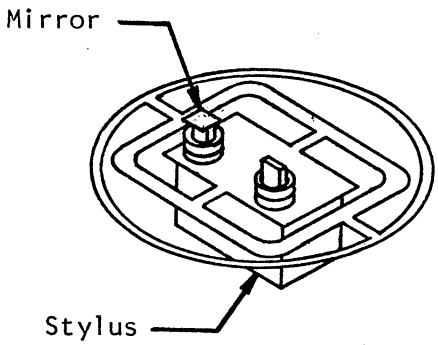

Figure 3. Stylus With Mirror Attached to Ferrite Core

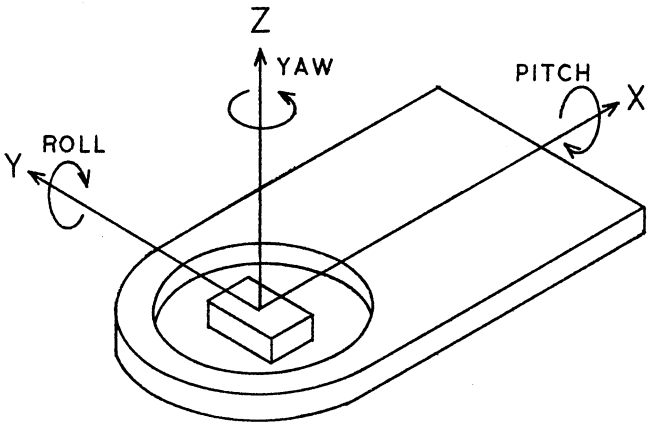

Figure 4. Definition of Degrees of Freedom Associated With Read/Write Head Displacements

lateral-effect photodiode to detect movement of the reflected beam. This system will be called the Linear Reflected Beam Analyzer (L-RBA). The The L-RBA system does not have the capability to separate stylus rotations and translations; however, this system will prove to be useful as an analysis tool.

The second system that is to be used is an extension of the L-RBA system. This second system splits the incoming laser beam into two separate coplanar beams. Both beams are directed at the mirror atop the stylus but each approaches at a different incident angle. This system requires the use of two detectors since there are two reflected beams. The use of two detectors allows for separation of beam motion caused by stylus rotation and vertical translation. The detectors used for this system are array (or two-axis) lateral-effect photodiodes. These detectors allow for detection of beam motion in two directions, thus allowing for simultaneous determination of stylus roll rotations along with the pitch rotation and vertical translation. This system will be called the Array Reflected Beam Analyzer (A-RBA).

Advantages and Disadvantages of the RBA Systems

The major advantage of the RBA systems is that they are noncontacting devices. The small size of the head system requires that the system used is to be as unobtrusive as possible. The mirror that must be affixed to the stylus for use of the RBA systems adds a small amount of mass to the slider and thus may change system response slightly; however, since the mass of the mirror is only a fraction of a percent of the total mass of the slider, these effects should be negligible. The lateral effect photodiodes that are used as beam motion detectors have a near

linear amplitude response if the reflected beam remains near the central portion of the detector. The RBA systems have an advantage over optical lever techniques which sense variation in reflected light intensity. Unlike other optical lever methods, the RBA systems can be configured such that pitch rotation, roll rotation, and vertical translation can be determined simultaneously. A disadvantage of the RBA system is the inability to examine motion of all six degrees of freedom of the stylus. A system capable of doing this would need a minimum of six data channels and calibration would be difficult. Two other disadvantages of the RBA systems are: first, all tests must be performed in a dark environment to reduce background noise; and second, flat frequency response is limited to 5 KHz by the amplifiers used in conjunction with the lateral-effect photodiodes. Other amplifiers are available which extend the frequency response to 30 KHz.

L-RBA System Equations

The equations developed in this section are based on the assumption that the read/write head stylus is essentially moving in only the pitch rotation, roll rotation, and vertical translation directions. The L-RBA system is configured such that it is most sensitive to these components of movement.

First consider the case of only a vertical translation of the stylus as depicted in Figure 5. The mirror is considered to be horizontal and the angle of incidence of the incoming laser beam measured from the horizontal is ψ; thus the angle of reflection is also ψ as measured from the horizontal. The detector is to be placed such that its surface is at a distance R from the initial position of the mirror and is set at an

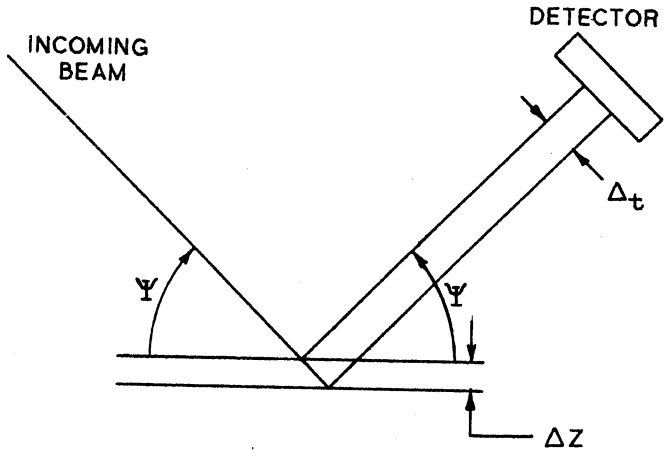

Figure 5. Reflected Beam Displacement Due to Vertical Translation

angle ψ from the vertical. This places the detector such that the reflected beam approaches from a direction normal to the face of the detector. If the stylus is translated by a distance Δ_z, it can be shown through use of simple geometry that the displacement Δ_t of the reflected beam is

$$\Delta_t = 2\Delta z \cos\psi \tag{2.1}$$

From Equation (2.1), it can be seen that the displacement of the position of the reflected beam is not dependent upon the distance from the mirror to the detector. Another significant factor is the dependence of the reflected beam displacement Δ_t on the incident angle of the incoming laser beam. In theory, if ψ were set to be 90 degrees, then the reflected beam would remain stationary and no translation could be detected; however, the system cannot be set for an incident angle of 90 degrees since the incoming beam would be required to pass through the detector. Equation (2.1) also reveals that the displacement of the reflected beam will be maximized as ψ approaches zero degrees, but this too is a physical impossibility.

Next, if the stylus is not allowed to translate but is rotated in the plane of the paper by an amount ϕ, as shown in Figure 6, the reflected beam will traverse across the face of the detector a distance Δ_ϕ which is found to be

$$\Delta_\phi = R \tan 2\phi \tag{2.2}$$

which for small angles ϕ is closely approximated by

$$\Delta_\phi = 2R\phi \tag{2.3}$$

The significance of Equations (2.2) and (2.3) is that unlike Δ_t, Δ_ϕ is independent of the incident angle ψ; however, Δ_ϕ is proportional to

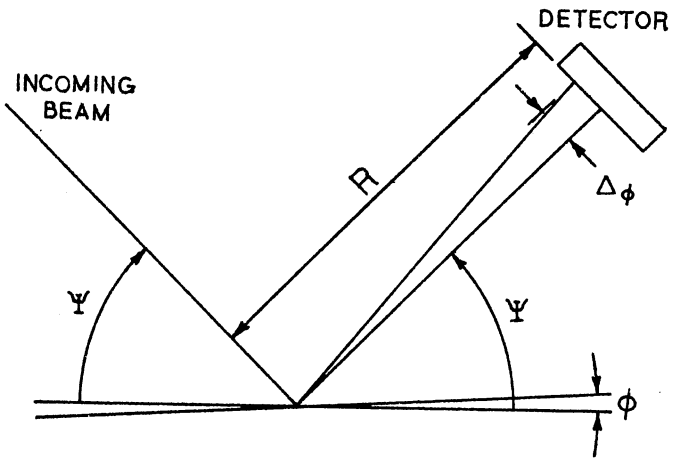

Figure 6. Reflected Beam Displacement Due to Rotation

the distance R between the mirror atop the stylus and the front surface of the detector. Since Δ_ϕ is proportional to the distance R, the L-RBA system can either be made very sensitive to stylus rotation by marking R large or it can be made essentially insensitive to rotations by making R very small.

The total displacement $\Delta_{\phi t}$ of the reflected beam due to both translation and rotation of the stylus is simply the superposition of Δ_ϕ and Δ_t, namely

$$\Delta_{\phi t} = \Delta_\phi + \Delta_t \tag{2.4}$$

Substituting Equations (2.1) and (2.3) into Equation (2.4) results in

$$\Delta_{\phi t} = 2R\phi + 2\Delta z \cos\psi \tag{2.5}$$

Equation (2.5) is based on the assumption that there are only two degrees of freedom associated with the movement of the stylus. It will be shown later that small motions in other directions will have an insignificant effect on the value of $\Delta_{\phi t}$ due to rotation and translation as depicted in Figures 5 and 6.

Since the L-RBA system allows for determination of only the quantity $\Delta_{\phi t}$, it is not possible to determine both Δ_ϕ and Δ_t simultaneously; however, either Δ_ϕ or Δ_t can be determined individually by selecting the proper values of ψ and R. If ψ is chosen to be as near to 90 degrees as is physically possible, then $\Delta_t << \Delta_\phi$ and $\Delta_{\phi t}$ is approximately equal to Δ_ϕ. Thus

$$\Delta_{\phi t} \tilde{=} 2R\phi \tag{2.6}$$

Equation (2.6) makes it possible to determine the stylus rotation ϕ from the value $\Delta_{\phi t}$, i.e.,

$$\phi = \frac{\Delta_{\phi t}}{2R} \tag{2.7}$$

If R is chosen to be very small and ψ is chosen such that it is not near 90 degrees, then $\Delta_{\phi} << \Delta_{t}$ and $\Delta_{\phi t}$ is approximately equal to Δ_{t}. Thus

$$\Delta_{\phi t} = 2\Delta z \cos\psi \tag{2.8}$$

Solving Equation (2.8) for Δ_{z} results in

$$\Delta z = \frac{\Delta_{\phi t}}{2\cos\psi} \tag{2.9}$$

The L-RBA system allows for determination of Δ_{ϕ} and Δ_{t} individually but does not allow for simultaneous calculation of these values. Also, the third motion component of interest (roll rotation θ) cannot be determined. More information must be known about the movement of the reflected beam in order to simultaneously determine Δ_{ϕ}, Δ_{t}, and Δ_{θ}. The A-RBA system was devised with these factors under consideration.

A-RBA System Equations

The A-RBA system is very similar to the L-RBA system. There are two main differences in these systems. First, the A-RBA system utilizes a beam splitter to produce two incoming beams as shown in Figure 7. This allows for separation of beam deflections into its components produced by pitch rotation and vertical translation. Second, the A-RBA system utilizes array lateral-effect photodiodes as detectors which make it possible to examine roll rotations simultaneously with the pitch rotations and vertical translation.

Consider a reflected beam $\vec{R}$ in the y-z plane as shown in Figure 8. If the stylus is rotated about the x-axis by an amount ϕ, the reflected

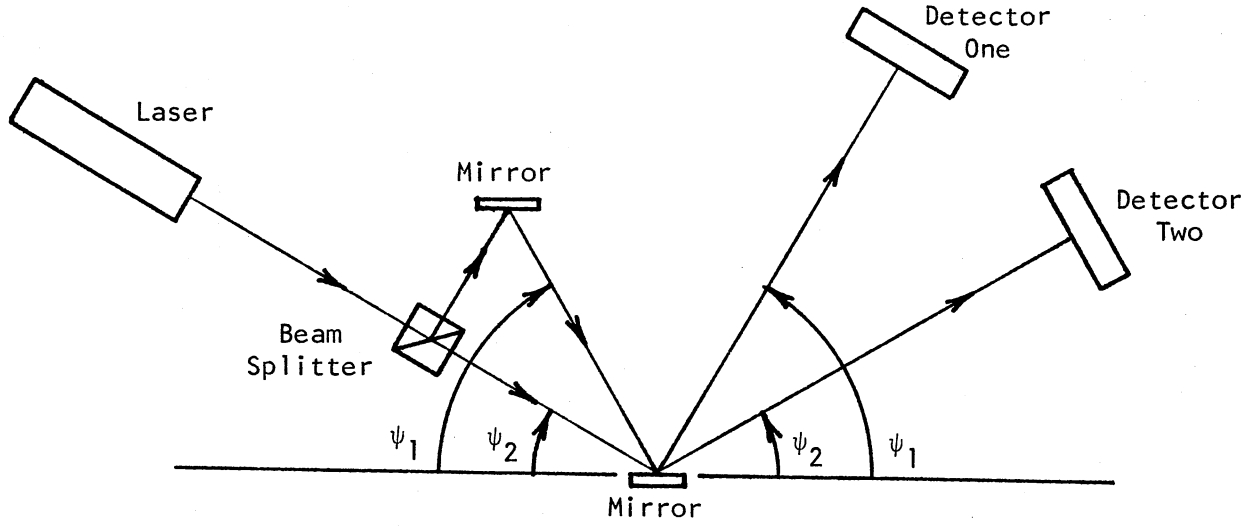

Figure 7. A-RBA System

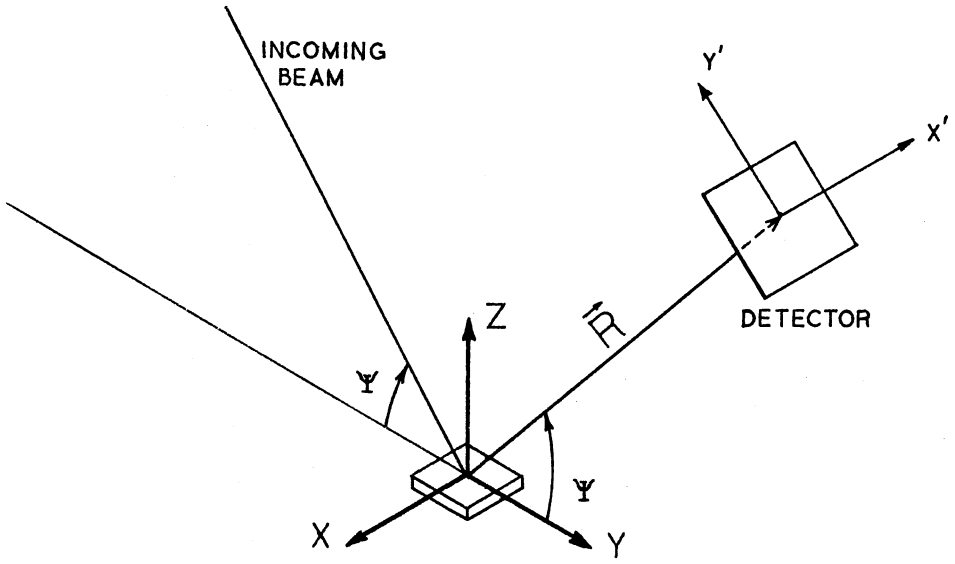

Figure 8. Reflected Beam $\vec{R}$ in the Y-Z Plane

beam is displaced from its initial angle ψ to a new direction which is at an angle of $\psi + 2\phi$. The displaced reflected beam can be broken into its x- and z-components:

$$\vec{R} = R\cos(\psi + 2\phi)\hat{i} + R\sin(\psi + 2\phi)\hat{k} \tag{2.10}$$

Now, if $\vec{R}$ is also rotated about the y-axis by an amount 2θ, which would represent the effect of rotating the stylus about the y-axis by an amount θ, the y-component of R is unaffected; however, the former z-component of Equation (2.10) now has a component in the x-direction as well as the z-direction. The final result of rotating $\vec{R}$ about the x- and y-axes by 2ϕ and 2θ, respectively, is

$$\vec{R} = R\cos(\psi + 2\phi)\hat{i} + R\sin(\psi + 2\phi)\sin 2\theta\hat{j} + R\sin(\psi + 2\phi)\cos 2\theta\hat{k} \tag{2.11}$$

The desired result of this derivation is the displacement of the end of the reflected beam as it is projected onto the face of the array detector, which is normal to the initial position of $\vec{R}$. The projection $\vec{P}$ of the displaced beam $\vec{R}$ onto the detector axes x' and y' can be shown to be

$$\vec{P} = R[\sin(\psi + 2\phi)\sin 2\theta]\hat{i}' - R[\sin(\psi + 2\phi)\cos 2\theta\cos\psi - \cos(\psi + 2\phi)\sin\psi]\hat{j}' \tag{2.12}$$

If the projection $\vec{P}$ is broken into its respective x'- and y'-components and these components renamed as follows,

$$\Delta_\theta = R\sin(\psi + 2\phi)\sin 2\theta\hat{i}' \tag{2.13}$$

$$\Delta_\phi = -R[\sin(\psi + 2\phi)\cos 2\theta\cos\psi - \cos(\psi + 2\phi)\sin\psi]\hat{j}' \tag{2.14}$$

then it can be shown that Equations (2.13) and (2.14) are the reflected beam displacements corresponding to pitch and roll rotations, respectively.

Expansion of Equation (2.14) results in

$$\Delta_\phi = R[(\sin\psi \cos 2\phi + \cos\psi \sin 2\phi) \cos 2\theta \cos\psi - (\cos\psi \cos 2\phi - \sin\psi \sin 2\phi) \sin\psi] \quad (2.15)$$

Since this technique will be used to examine rotations of very small amplitude, the small angle approximations

$$\sin 2\phi \tilde{=} 2\phi \quad (2.16a)$$

$$\cos 2\phi \tilde{=} 1 \quad (2.16b)$$

$$\sin 2\theta \tilde{=} 2\theta \quad (2.16c)$$

$$\cos 2\theta \tilde{=} 1 \quad (2.16d)$$

would be valid. After substituting Equations (2.16a) through (2.16d), Equation (2.15) reduces to

$$\Delta_\phi = R[\sin\psi \cos\psi + 2\phi\cos^2\psi - \sin\psi \cos\psi + 2\phi\sin^2\psi] \quad (2.17)$$

which is simply

$$\Delta_\phi = 2R\phi \quad (2.18)$$

Equation (2.13) can be similarly reduced to

$$\Delta_\theta = 2R\theta\sin\psi + (2\phi)(2\theta) \cos\psi \quad (2.19)$$

Since 2ϕ and 2θ are both small terms, the $\cos\psi(2\phi)(2\theta)$ term is very small compared to the $2R\theta\sin\psi$ term; thus

$$\Delta_\theta \tilde{=} 2R\theta\sin\psi \quad (2.20)$$

It can be seen that Equations (2.18) and (2.20) represent the reflected beam displacements due to pitch rotation ϕ and roll rotation θ, respectively.

The beam displacement due to vertical translation only is given in Equation (2.1). Equation (2.1) was derived for the L-RBA system, but the

same relation is applicable for the y'-axis of both detectors of the A-RBA system. Superposition of Equations (2.1) and (2.18) will yield the total reflected beam displacement $\Delta_{\phi t}$ in the y'-direction:

$$\Delta_{\phi t} = 2R\phi + 2\Delta z \cos\psi \tag{2.21}$$

Note that this is exactly the same as Equation (2.5).

Recall that the A-RBA system has two detectors that are placed at different angles (Figure 7) and thus Equations (2.20) and (2.21) are applicable for both detectors, each with its own value of ψ. The entire system of equations for the A-RBA system is as follows:

$$\Delta_{\phi t1} = 2R\phi + 2\Delta z \cos\psi_1 \tag{2.22a}$$

$$\Delta_{\theta 1} = 2R\theta \sin\psi_1 \tag{2.22b}$$

$$\Delta_{\phi t2} = 2R\phi + 2\Delta z \cos\psi_2 \tag{2.22c}$$

$$\Delta_{\theta 2} = 2R\theta \sin\psi_2 \tag{2.22d}$$

Subtracting Equation (2.22c) from (2.22a) and solving for Δz produces the relationship which allows for separation of the vertical translation and pitch rotation:

$$\Delta z = \frac{\Delta_{\phi t1} - \Delta_{\phi t2}}{2(\cos\psi_1 - \cos\psi_2)} \tag{2.23}$$

Substitution of Equation (2.23) into (2.22a) and (2.22c) will yield two equally valid solutions for the pitch rotation ϕ:

$$\phi = \frac{\Delta_{\phi t1}}{2R} - \frac{[\Delta_{\phi t1} - \Delta_{\phi t2}]\cos\psi_1}{2R[\cos\psi_1 - \cos\psi_2]} \tag{2.24a}$$

$$= \frac{\Delta_{\phi t2}}{2R} - \frac{[\Delta_{\phi t1} - \Delta_{\phi t2}]\cos\psi_2}{2R[\cos\psi_1 - \cos\psi_2]} \tag{2.24b}$$

The roll rotation θ can be calculated from either Equation (2.22b) or (2.22d):

$$\theta = \frac{\Delta_{\theta 1}}{2R\sin\psi_1} \tag{2.25a}$$

$$\theta = \frac{\Delta_{\theta 2}}{2R\sin\psi_2} \tag{2.25b}$$

Equations (2.23), (2.24), and (2.25) show that in theory the A-RBA system will allow for simultaneous calculation of the pitch rotation, roll rotation, and vertical translation of the read/write head stylus.

Calibration of L-RBA System

The L-RBA system was calibrated by determining the sensitivity of the linear lateral-effect photodiode that is used to detect the displacement of the reflected beam. The photodiode used is a model LSC-5D which is manufactured by United Detector Technology (UDT). The photodiode was used in conjunction with a UDT model 301-DIV transimpedance (current-to-voltage) amplifier. The sensitivity will be defined as the output voltage (volts) of the photodiode-amplifier system for a unit displacement (one inch) of the laser beam striking the detector face. A sketch of the LSC-5D photodiode is shown in Figure 9. The active area of the photodiode (shaded portion in Figure 9) measures 0.085 inches wide by 0.2 inches long.

A lateral-effect photodiode produces a current which is proportional to the distance from the null position of the detector (near the detector center in the longitudinal direction) to the centroid of the beam which is striking the active area. A beam displacement to one side of the null

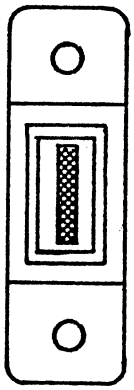

Figure 9. UDT LSC-5D Lateral-Effect Photodiode

position produces a positive current and a beam displacement to the other side produces a negative current. The 301-DIV amplifier produces an output voltage which is proportional to the current produced by the photodiode. Thus the beam displacement can be determined by monitoring the output voltage if the sensitivity of the photodiode-amplifier system is known.

Static Calibration of Photodiode-Amplifier System

The sensitivity of the photodiode-amplifier system was examined by affixing the photodiode to a micrometer table and directing a laser beam at its face. The photodiode could then be moved by precisely adjusting the position of the micrometer table. The laser beam remains stationary; thus adjustment of the micrometer table produces a relative beam displacement at the face of the detector.

The table was initially adjusted so that the centroid of the laser beam was positioned at the null position of the photodiode. This produced a zero output voltage from the amplifier. The micrometer table was then adjusted in 0.020 inch increments and the output voltages were recorded. This procedure was repeated until the entire active area had been traversed. The results of this procedure are given in Table I. The sensitivity of the photodiode-amplifier system was calculated from the output voltages given in Table I by using a fourth-order central difference scheme [16]. Note that sensitivity could not be calculated for the first and last two points using this procedure. Figure 10 is a plot of output voltage versus beam displacement from the null position of the photodiode. Inspection of Figure 10 and the calculated sensitivities of Table I show that the photodiode is not linear throughout its entire

TABLE I

OUTPUT VOLTAGES AND SENSITIVITIES OBTAINED FROM STATIC CALIBRATION OF THE LINEAR LATERAL-EFFECT PHOTODIODE

Beam Displacement (Inches)	Output Voltage (Volts)	Calculated Sensitivity (Volts/Inch)
-0.120	-8.093	---
-0.100	-7.029	---
-0.080	-5.957	56.80
-0.060	-4.757	58.79
-0.040	-3.552	70.44
-0.020	-1.899	90.40
0.000	0.000	97.09
0.020	1.961	102.42
0.040	4.026	---
0.060	5.728	---

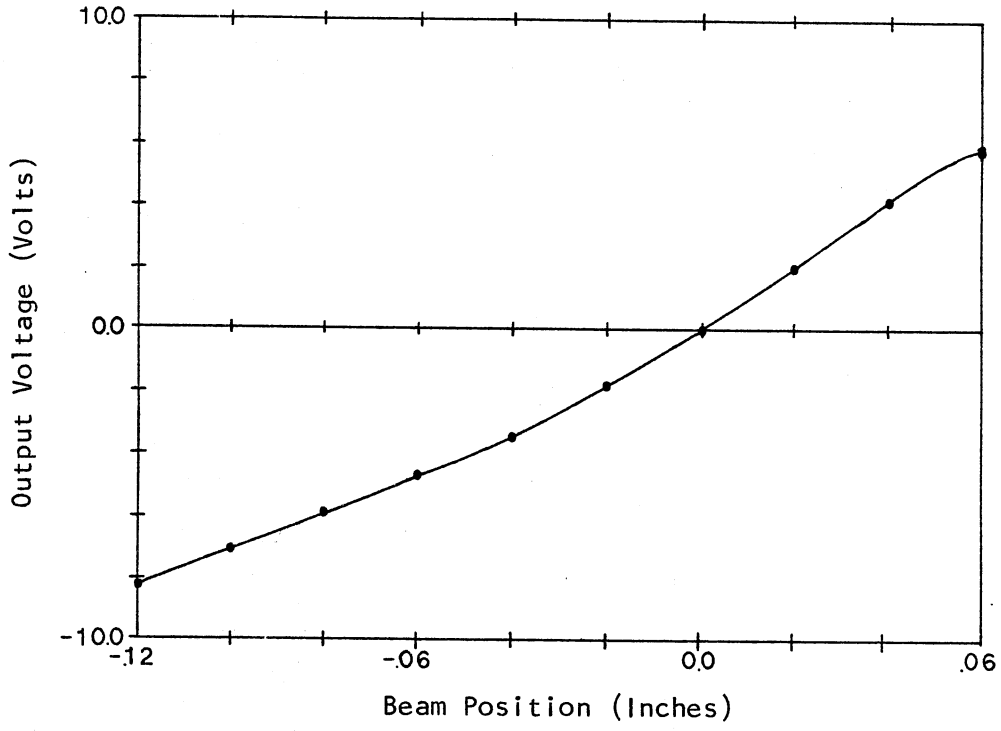

Figure 10. Output Voltage Versus Beam Position for Linear Lateral-Effect Photodiode

range, but the output voltages are nearly linear if the beam remains near the null position.

Dynamic Calibration of the L-RBA System Using Pure Rotation

The mechanism shown in Figure 11 was used to calibrate the L-RBA system using pure rotation. The free bar was driven by a MB Electronics electromagnetic shaker. Movement of the free bar causes the connecting arms to rotate about the pivot. The pin which is used as a pivot is fixed to the connecting arms; thus the pin rotates also. A transverse notch was machined in the pin to allow for placement of a small mirror at the center of rotation. The free bar was driven sinusoidally at a zero-to-peak amplitude of 0.00127 inches. Referring to Equation (2.6), the distance R was set to be 42.25 inches (the maximum allowed by system construction). The connecting arms are two inches long; thus a 0.00127 inch zero-to-peak translation of arm B causes a peak-to-peak rotation of 0.00127 radians. Using these values, $\Delta_{\phi t}$ of Equation (2.6) is calculated to be 0.1073 inches. This value is the peak-to-peak beam displacement at the face of the detector.

This portion of the calibration procedure was performed for only one displaced beam amplitude (0.1073 inches) at frequencies of 5, 10, 25, 50, 100, 150, and 200 Hz. The maximum frequency used was limited by the capacity of the electromagnetic shaker. It would be desirable to obtain calibration data for frequencies up to 5 KHz, but this was not feasible with the equipment available. The photodiode is reported to have a rise time (10 to 90%) of 500 ns, which is far less than the 200,000 ns period of a 5 KHz signal. Thus the photodiode should maintain flat frequency response

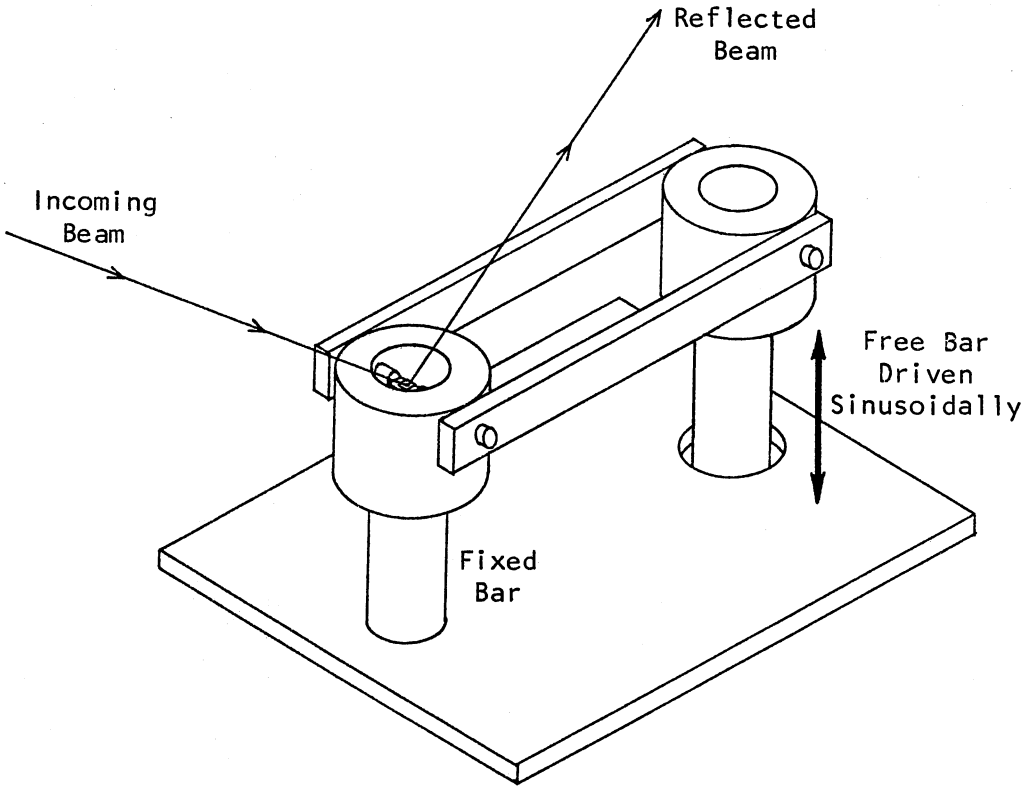

Figure 11. Mechanism Used to Calibrate L-RBA System Using Pure Rotation

well beyond the maximum to be used in this analysis. The UDT 301-DIV amplifier is rated at a maximum 3 dB dropoff at 5 KHz.

The output signal from the amplifier was monitored using a Spectral Dynamics model SD 345 real time analyzer. A minimum of five sets of data were taken for each of the above mentioned frequency settings. The average and standard deviation of the output voltages obtained from the data sets are given in Table II. Also shown in Table II are the sensitivities obtained by dividing the output voltage by 0.1073 inches. Figure 12 is a plot of the output voltages versus excitation frequency. The error bands shown are placed at ±2 standard deviations which for a Gaussian distribution would contain about 95 percent of all values. The average of the sensitivity values of Table II is 70.81 volts/inch. This value will be used for comparison with static calibration efforts and the pure vertical translation calibration of the next section.

Dynamic Calibration of L-RBA System Using Pure Vertical Translation

Figure 13 depicts the mechanism that was used to calibrate the L-RBA system using pure vertical translation. A mirror was mounted on top of the bar which is extended from the head of the electromagnetic shaker. The laser beam strikes the mirror and is reflected to the photodiode. For these tests the photodiode was placed at 2.375 inches from the mirror, since much error was encountered with a separation of 42.25 inches between the mirror and photodiode. The error was induced by a rocking motion of the bar in addition to the vertical translation (refer to Equations (2.4) and (2.5)).

TABLE II

PEAK-TO-PEAK OUTPUT VOLTAGES FROM L-RBA SYSTEM CALIBRATION FOR A PEAK-TO-PEAK ROTATION AMPLITUDE OF 0.00127 RADIANS

Excitation Frequency (Hz)	Mean Output Voltage (Volts)	Standard Deviation of Output Voltage (Volts)	Calculated Photodiode Sensitivity (Volts/Inch)
5.0	7.527	0.126	70.15
10.0	7.414	0.101	69.08
25.0	7.619	0.153	71.01
50.0	7.465	0.264	69.57
100.0	7.513	0.180	70.02
150.0	7.627	0.342	71.08
200.0	7.968	0.345	74.26

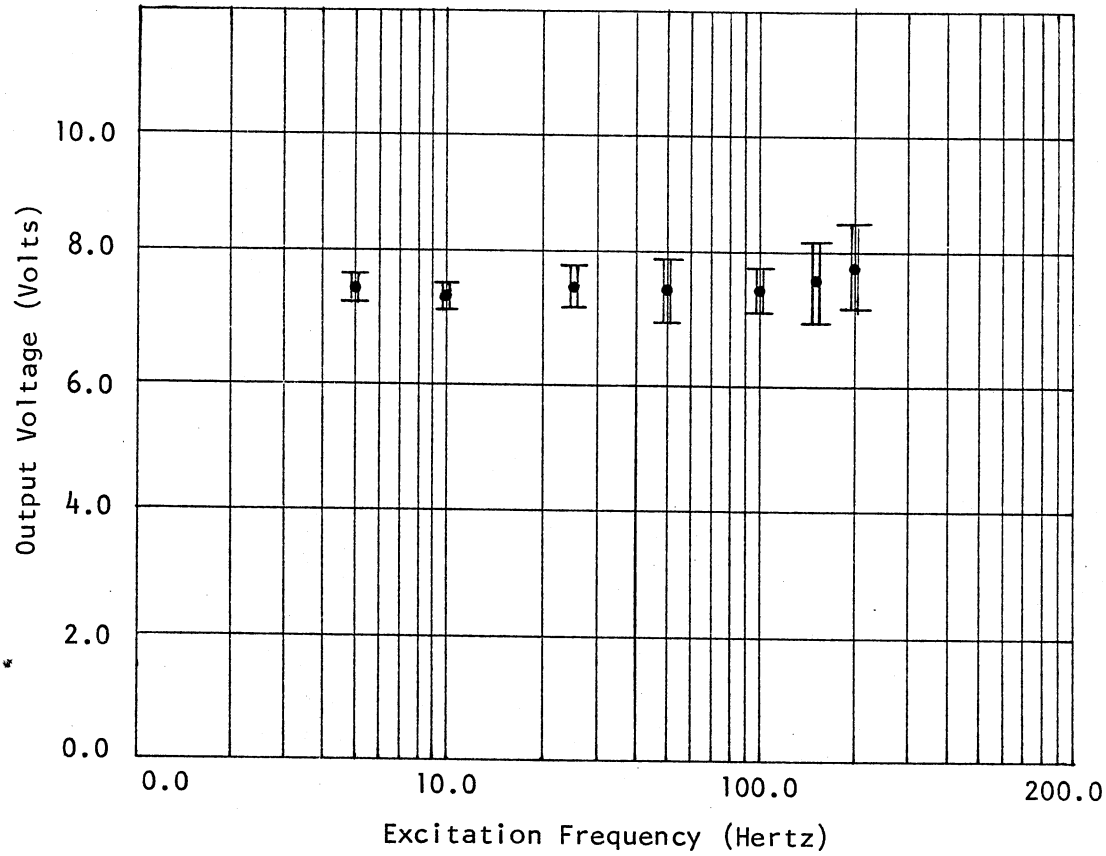

Figure 12. Output Voltage Versus Excitation Frequency for the L-RBA System Subjected to a Mirror Rotation of 0.00127 Radians

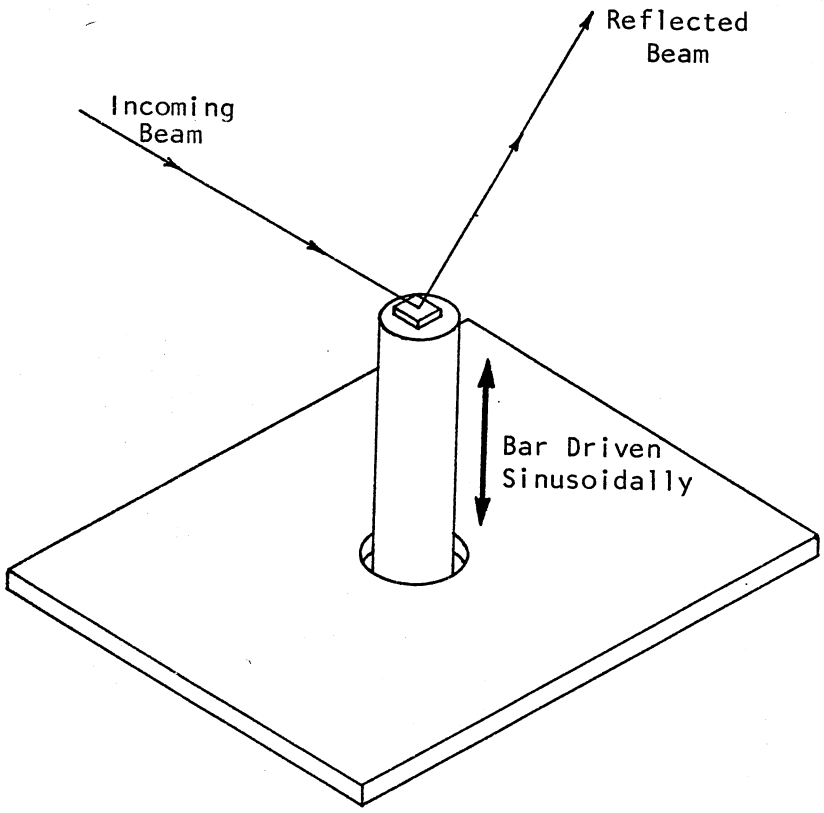

Figure 13. Mechanism Used to Calibrate L-RBA System Using Vertical Translation

This portion of the L-RBA system calibration was performed at an excitation frequency of 45 Hz for five vertical translation amplitude settings and for five incident beam angles. The translation amplitude values ranged from 0.00141 to 0.0318 inches. The incident beam angle (see Equation (2.8)) was set at values ranging from 29 to 81 degrees. The results of the tests as well as the calculated sensitivities are given in Table III. A plot of the output voltages resulting from this procedure is shown in Figure 14. The sensitivity is found by dividing the peak-to-peak output voltage by twice the zero-to-peak distance $\Delta_{\phi t}$, which is calculated using Equation (2.8) and the appropriate value of ψ. Statistical analysis of the sensitivity values of Table III reveals that the average sensitivity as found from vertical translation only is 65.55 volts/inch with a standard deviation of 4.72 volts/inch.

Summary of L-RBA System Calibration

The linear lateral-effect photodiode was found to have flat frequency response up to the test limitation of 200 Hz. The amplitude response is not ideal for large displacements; however, this presents no problem if the beam is not displaced far from the null position of the photodiode. The pure rotation calibration procedure revealed an average sensitivity of 70.81 volts/inch. The vertical translation calibration gave an average sensitivity of 65.55 volts/inch; thus there is a 7.4 percent difference in the two calculated sensitivities found in the dynamic testing. Static calibration revealed that sensitivity varies with respect to distance from the null position. From Figure 10, it is evident that the null position is not in the center of the active area. In actuality, it appears to be about 0.04 inches to the left of the null position (as

TABLE III

OUTPUT VOLTAGES FROM L-RBA SYSTEM CALIBRATION
USING VERTICAL TRANSLATION

Incident Angle ψ (Degrees)	Zero-to-Peak Translation Amplitude (Inches)	Peak-to-Peak Output Voltage (Volts)	Calculated Photodiode Sensitivity (Volts/Inch)
29.0	0.01767	3.600	57.84
	0.00707	1.537	61.83
	0.00354	0.742	59.69
	0.00141	0.299	60.14
45.0	0.03182	5.480	61.09
	0.02122	3.907	65.39
	0.00707	1.414	70.98
	0.00354	0.677	67.94
	0.00141	0.273	68.42
61.0	0.03182	3.918	61.56
	0.02122	2.734	66.44
	0.00707	0.935	68.14
	0.00354	0.466	67.96
	0.00141	0.185	67.59
70.0	0.03182	2.719	60.99
	0.02122	1.879	64.33
	0.00707	0.654	66.02
	0.00354	0.297	59.96
	0.00141	0.118	59.56
81.0	0.03182	1.468	69.87
	0.02122	1.008	71.97
	0.00707	0.345	73.89
	0.00354	0.162	69.57
	0.00141	0.067	72.13

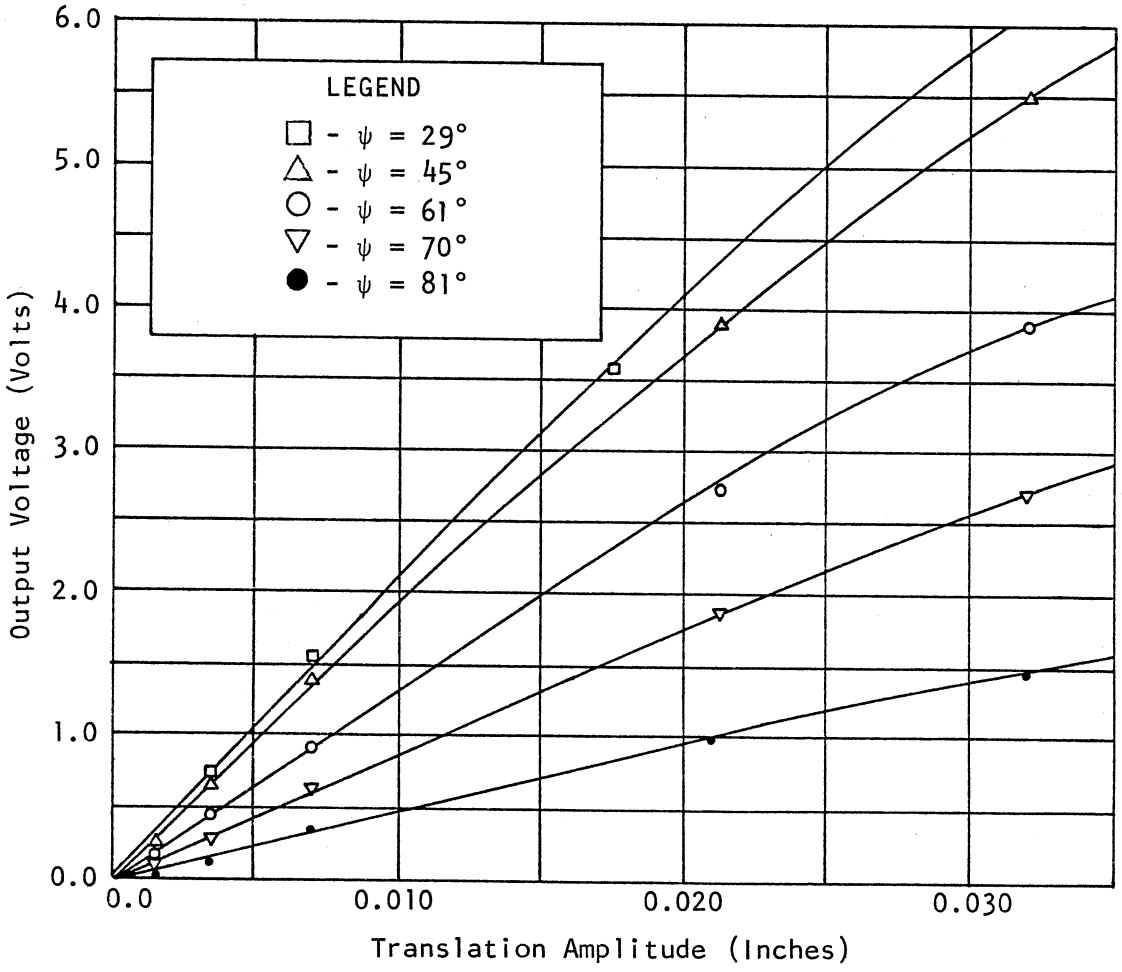

Figure 14. Output Voltage Versus Translation Amplitude for the L-RBA System Set at Various Incident Angles

referenced in Figure 10). This is an important detail as all calibration data and subsequent test data were obtained with the operating point chosen to be in the physical center of the lateral-effect photodiode. This was done for the sake of a convenient reference point for system setup. Note that the sensitivity at a point 0.04 inches to the left of null (-0.04 inches) as calculated from static calibration data is 70.44 volts/inch. This agrees very well with the 70.81 volt/inch sensitivity found in dynamic calibration using pure rotation. It will be assumed that the photodiode sensitivities found using pure vertical translation could be slightly in error due to system sensitivity to geometric factors. A sensitivity of 71 volts/inch will be used for data reduction purposes. This value will be sufficient for two-digit accuracy which is the maximum that can be assumed to be reliable.

Calibration of A-RBA System

Calibration of the A-RBA system proved to be a difficult task. This system uses array (two-axis) lateral-effect photodiodes as beam deflection sensors. The array photodiodes used in the A-RBA system are the UDT model PIN-SC/10D. Each of these photodiodes requires the use of two UDT 301-DIV transimpedance amplifiers. A sketch representing one of these photodiodes is shown in Figure 15. Referring to Figure 7, the A-RBA system is constructed such that R is set at 35 inches for both detectors, and there is a fixed angle of 20 degrees separating detector one and detector two. The system was adjusted for incident beam angles of 48.5 and 68.5 degrees (fixed 20 degree separation) at detectors one and two, respectively. The design of the system does not allow for values of R

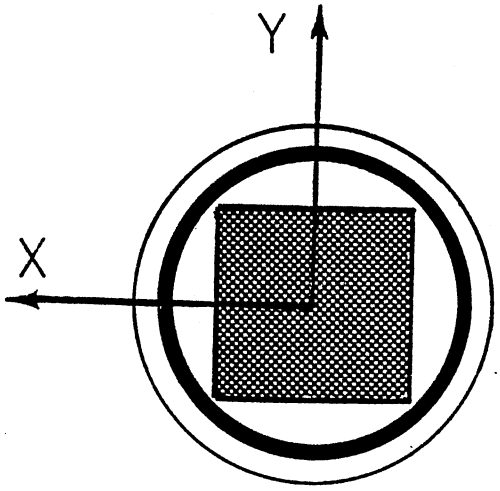

Figure 15. UDT PIN-SC/10D Two-Axis Lateral-Effect Photodiode

other than 35 inches. This arrangement allows for high sensitivity to both pitch and roll rotations due to the selected value of R.

Two major problems were encountered in attempts at dynamic calibration. First, the electromagnetic shaker that was used for dynamic calibration of the L-RBA system was not functioning properly; thus it could not be used and a suitable replacement was not available. Second, an attempt was made to calibrate for pure vertical translation using a small portable shaker; however, the shaft of this shaker rocked slightly as it translated, resulting in large errors due to the system's high sensitivity to rotations. This is the same problem that was encountered with calibration of the L-RBA system, but the A-RBA system does not allow for a reduced value of R. In view of these problems, dynamic calibration attempts were discontinued and static tests were performed. The results of the L-RBA system calibration reveal that static calibration should be sufficient for finding the sensitivity of the array photodiodes.

Static Calibration of the Array Lateral-Effect Photodiodes

The sensitivity of the array photodiodes was determined in much the same way as the linear photodiodes. Each of the photodiodes was attached to a two-axis micrometer table and a laser beam was directed at its front surface. Since the array detectors are two-axis devices, each requires use of two UDT 301-DIV amplifiers. The axes of the photodiodes (see Figure 15) were aligned with the axes of the micrometer table. The table was adjusted until the voltage output from both axes read near zero volts, thus indicating that the beam was centered on the null position in both directions. The entire 0.4- by 0.4-inch surface of both photo-

diodes was examined using 0.040-inch increments in both axis directions. Note that actually only a 0.32- by 0.32-inch area was examined, as this is the maximum area that can be examined with the entire beam contained inside the active area of the photodiode. The results obtained from this procedure are presented in Tables IV through VII. Plots of the data taken along the x- and y-axes (null position for the y- and x-directions, respectively) of the photodiodes are shown in Figures 16 and 17. Inspection of these results reveals that, like the linear photodiode, the array photodiodes are nonlinear (with respect to beam displacement) toward the edges; however, if the beam remains in the central 25 percent area of the photodiode, acceptable linearity results. The data in Tables IV through VII also reveal that the voltage output from the x-axis of the photodiode for a given beam position in the x-direction will be essentially the same regardless of the y-position of the beam; likewise, the converse is true for the voltage output of the y-axis of the photodiode for a given beam position in the y-direction. Tables VIII and IX contain the average and standard deviation of all output voltages of the x- and y-axes for a given displacement in the respective axis direction. Note that these values are for the central 25 percent portion of the active area. Table VIII contains the data for detector one and Table IX contains the data for detector two.

The sensitivities are denoted as S_{ij} where the i subscript will represent either a one or a two, thus indicating whether it is for photodiode number one or number two and the subscript j will represent either an x or a y denoting sensitivity for either the x-axis or the y-axis. The respective sensitivities were calculated using the least squares method modified such that the linear fit is required to pass through the

TABLE IV

OUTPUT VOLTAGES (IN VOLTS) FROM X-AXIS OF ARRAY DETECTOR ONE FOR BEAM POSITIONED AT A POINT (X,Y) ON THE DETECTOR FACE

Beam Position From Null in Y-Direction (In.)	Beam Position From Null in X-Direction (Inches)								
	-0.160	-0.120	-0.080	-0.040	+0.00	+0.040	+0.080	+0.120	+0.160
+0.160	+9.05	+8.00	+6.07	+3.32	+0.28	-2.90	-5.76	-7.90	-9.04
+0.120	+8.90	+7.78	+5.81	+3.20	+0.00	-2.85	-5.67	-7,74	-8.90
+0.080	+8.77	+7.65	+5.66	+3.17	+0.00	-2.84	-5.56	-7.60	-8.79
+0.040	+8.70	+7.52	+5.60	+3.08	+0.00	-2.80	-5.51	-7.57	-8.73
+0.000	+8.65	+7.45	+5.50	+3.00	+0.00	-2.99	-5.65	-7.60	-8.75
-0.040	+8.70	+7.50	+5.52	+3.00	+0.00	-3.08	-5.74	-7.68	-8.79
-0.080	+8.79	+7.66	+5.68	+2.95	+0.00	-3.20	-5.92	-7.86	-8.90
-0.120	+8.92	+7.82	+5.83	+3.10	+0.00	-3.36	-6.10	-8.00	-9.05
-0.160	+9.07	+7.98	+5.96	+3.08	-0.02	-3.50	-6.22	-8.20	-9.18

TABLE V

OUTPUT VOLTAGES (IN VOLTS) FROM Y-AXIS OF ARRAY DETECTOR ONE FOR BEAM POSITIONED AT A POINT (X,Y) ON THE DETECTOR FACE

Beam Position From Null in Y-Direction (In.)	Beam Position From Null in X-Direction (Inches)								
	-0.160	-0.120	-0.080	-0.040	+0.00	+0.040	+0.080	+0.120	+0.160
+0.160	+8.83	+8.70	+8.58	+8.50	+8.50	+8.55	+8.63	+8.76	+8.92
+0.120	+7.60	+7.46	+7.30	+7.25	+7.20	+7.28	+7.41	+7.58	+7.77
+0.080	+5.55	+5.50	+5.38	+5.30	+5.32	+5.38	+5.52	+5.61	+5.70
+0.040	+2.70	+2.78	+2.75	+2.81	+2.85	+2.84	+2.87	+2.91	+2.91
+0.000	-0.30	-0.18	-0.10	-0.00	+0.00	+0.00	-0.10	-0.20	-0.30
-0.040	-3.62	-3.48	-3.20	-3.20	-3.15	-3.18	-3.30	-3.48	-3.60
-0.080	-6.29	-6.10	-5.90	-5.80	-5.75	-5.83	-5.94	-6.18	-6.36
-0.120	-8.13	-7.95	-7.73	-7.65	-7.62	-7.67	-7.80	-8.00	-8.18
-0.160	-9.06	-8.92	-8.78	-8.70	-8.70	-8.73	-8.83	-8.98	-9.12

TABLE VI

OUTPUT VOLTAGES (IN VOLTS) FROM X-AXIS OF ARRAY DETECTOR TWO FOR BEAM POSITIONED AT A POINT (X,Y) ON THE DETECTOR FACE

Beam Position From Null in Y-Direction (In.)	Beam Position From Null in X-Direction (Inches)								
	-0.160	-0.120	-0.080	-0.040	+0.00	+0.040	+0.080	+0.120	+0.160
+0.160	+9.22	+8.35	+6.58	+3.89	+0.67	-2.59	-5.60	-7.83	-9.07
+0.120	+9.07	+8.13	+6.33	+3.61	+0.45	-2.67	-5.50	-7.67	-8.91
+0.080	+8.91	+7.87	+5.98	+3.30	+0.25	-2.74	-5.45	-7.48	-8.74
+0.040	+8.80	+7.73	+5.78	+3.14	+0.00	-2.79	-5.38	-7.37	-8.64
+0.000	+8.77	+7.67	+5.70	+3.00	+0.00	-2.86	-5.45	-7.40	-8.62
-0.040	+8.76	+7.66	+5.68	+3.00	-0.03	-3.00	-5.56	-7.50	-8.68
-0.080	+8.84	+7.72	+5.71	+2.96	-0.09	-3.08	-5.66	-7.64	-8.82
-0.120	+8.97	+7.90	+5.90	+3.05	-0.13	-3.19	-5.85	-7.84	-8.97
-0.160	+9.14	+8.12	+6.10	+3.13	-0.14	-3.35	-6.00	-8.00	-9.12

TABLE VII

OUTPUT VOLTAGES (IN VOLTS) FROM Y-AXIS OF ARRAY DETECTOR TWO FOR BEAM POSITIONED AT A POINT (X,Y) ON THE DETECTOR FACE

Beam Position From Null in Y-Direction (In.)	Beam Position From Null in X-Direction (Inches)								
	-0.160	-0.120	-0.080	-0.040	+0.00	+0.040	+0.080	+0.120	+0.160
+0.160	+9.01	+8.92	+8.81	+8.70	+8.67	+8.69	+8.77	+8.88	+9.03
+0.120	+8.06	+7.95	+7.72	+7.59	+7.50	+7.50	+7.60	+7.80	+8.02
+0.080	+6.19	+5.95	+5.80	+5.65	+5.58	+5.56	+5.62	+5.80	+6.05
+0.040	+3.40	+3.30	+3.25	+3.13	+3.09	+3.05	+3.09	+3.20	+3.30
+0.000	-0.06	+0.00	+0.06	+0.00	+0.00	+0.00	+0.00	+0.00	+0.00
-0.040	-3.22	-3.10	-3.00	-2.91	-2.92	-2.91	-2.88	-3.00	-3.00
-0.080	-5.95	-5.79	-5.61	-5.50	-5.42	-5.43	-5.48	-5.54	-5.66
-0.120	-7.88	-7.69	-7.52	-7.36	-7.30	-7.32	-7.41	-7.54	-7.68
-0.160	-8.92	-8.80	-8.65	-8.55	-8.50	-8.50	-8.57	-8.70	-8.81

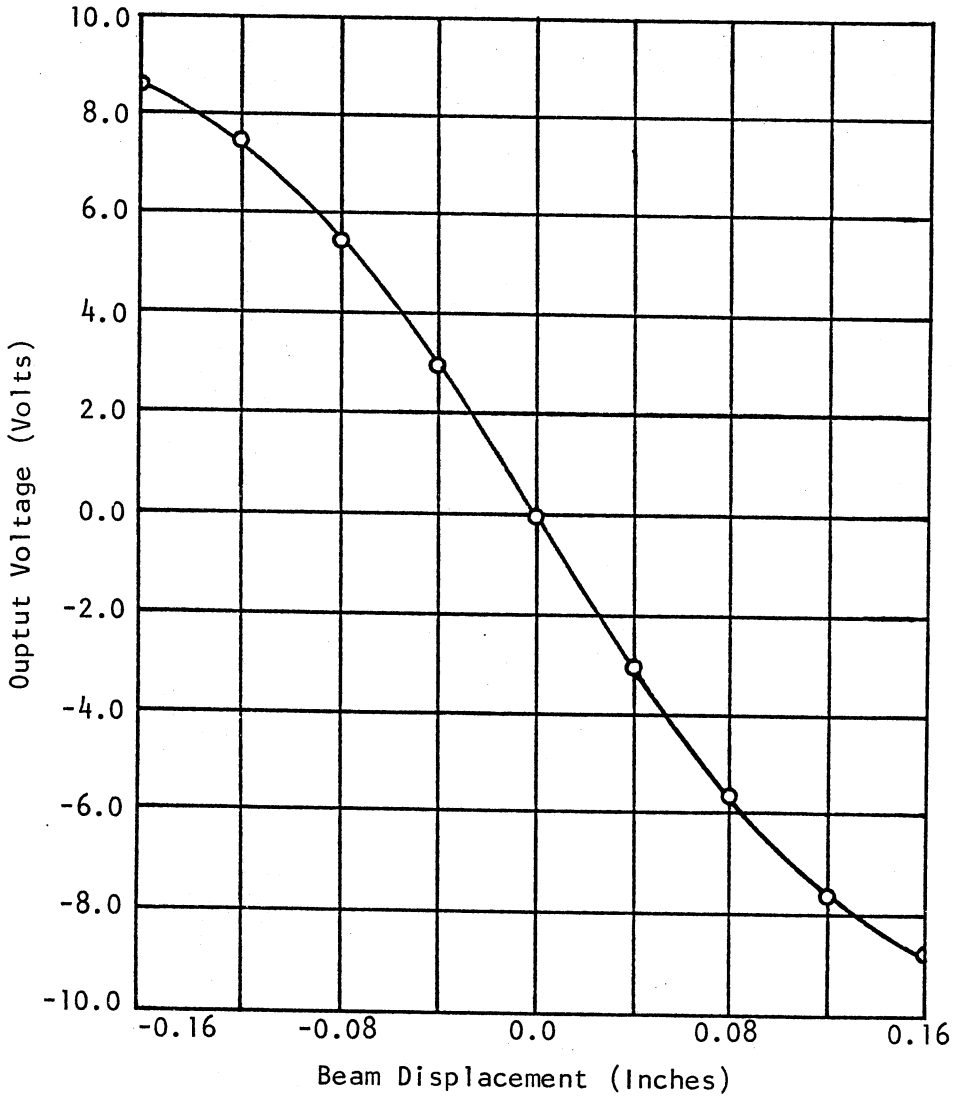

Figure 16. Output Voltage Versus Beam Displacement Along the Null X-Axis of Array Photodiode (Detector One)

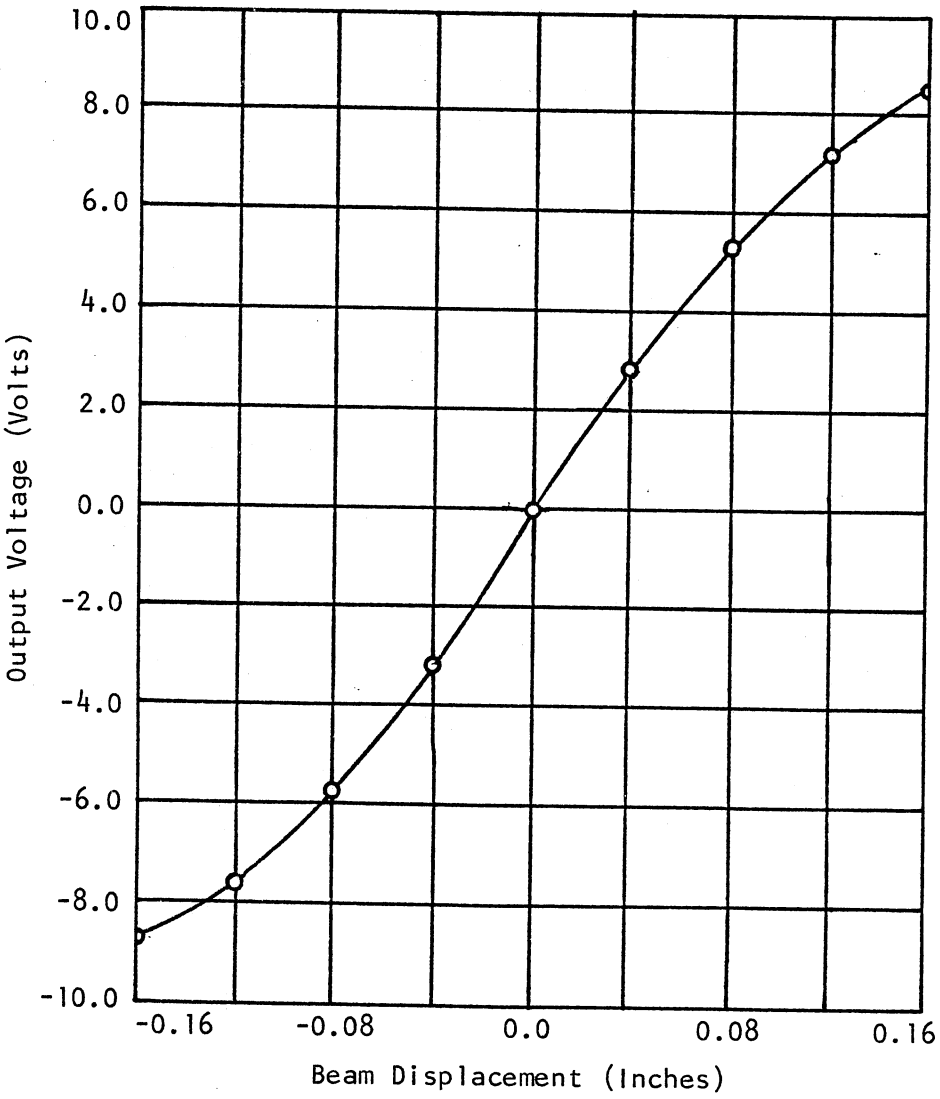

Figure 17. Output Voltage Versus Beam Displacement Along the Null Y-Axis of Array Photodiode (Detector One)

TABLE VIII

AVERAGE OUTPUT VOLTAGE FROM DETECTOR ONE FOR A GIVEN BEAM POSITION IN THE X- AND Y- DIRECTIONS (CENTRAL 25 PERCENT AREA ONLY)

X-Position (Inches)	$\bar{V}_x$ (Volts)	σ (V_x) (Volts)	Y-Position (Inches)	$\bar{V}_y$ (Volts)	σ (V_y) (Volts)
0.08	-5.76	0.16	0.08	5.38	0.09
0.04	-2.98	0.17	0.04	2.82	0.05
0.00	0.00	0.00	0.00	0.00	0.00
-0.04	3.04	0.09	-0.04	-3.21	0.06
-0.08	5.59	0.08	-0.08	-5.84	0.08

TABLE IX

AVERAGE OUTPUT VOLTAGE FROM DETECTOR TWO FOR A GIVEN BEAM POSITION IN THE X- AND Y- DIRECTIONS (CENTRAL 25 PERCENT AREA ONLY)

X-Position (Inches)	$\bar{V}_x$ (Volts)	σ (V_x) (Volts)	Y-Position (Inches)	$\bar{V}_y$ (Volts)	σ (V_y) (Volts)
0.08	-5.50	0.11	0.08	5.64	0.09
0.04	-2.89	0.14	0.04	3.12	0.08
0.00	0.00	0.00	0.00	0.00	0.00
-0.04	3.08	0.14	-0.04	-2.92	0.05
-0.08	5.77	0.12	-0.08	-5.49	0.08

origin. Using this method and the data in Tables VIII and IX, the sensitivities are calculated using the relation

$$S_{ij} = \sum_{n=1}^{5} \frac{(\Delta_{ij}\ \bar{V}_{ij})_n}{(\Delta_{ij})_n^2} \tag{2.26}$$

where $(\Delta_{ij})_n$ is the displacement from the null position of detector i in direction j, and $(\bar{V}_{ij})_n$ is the average output voltage corresponding to $(\Delta_{ij})_n$. The results of these calculations are:

$$S_{1x} = -71.80 \text{ V/in.}$$

$$S_{1y} = 71.18 \text{ V/in.}$$

$$S_{2x} = -71.28 \text{ V/in.}$$

$$S_{2y} = 70.75 \text{ V/in.}$$

The difference in sign of x- and y-sensitivities is due to the displacement direction assumed to be positive. Figure 18 is a plot of the average output voltages for photodiode number one in the x-direction (central 25 percent portion only). The line constructed through the data points has a slope which is equal to sensitivity S_{1x}. Similar results are evident for the y-axis as well. For test data reduction purposes, all sensitivities (S_{1x}, S_{1y}, S_{2x}, S_{2y}) will be assumed to be 71 volts/inch (neglecting sign). If dynamic amplitude and frequency response could have been examined, it is expected that similar sensitivities would be obtained.

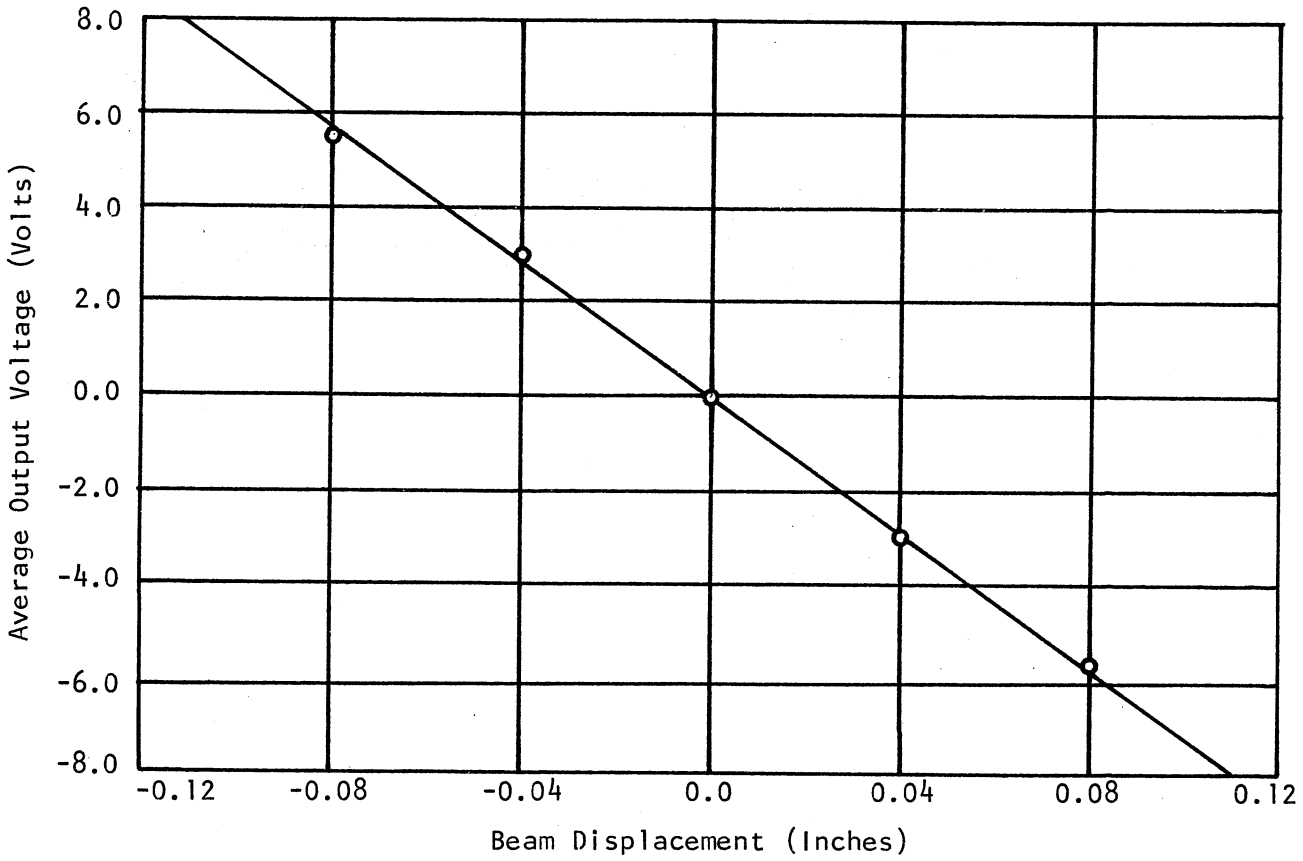

Figure 18. Average Output Voltage Versus Beam Displacement in X-Direction for Central 25 Percent Portion of Array Photodiode (Detector One)

CHAPTER III

EXPERIMENTAL PROCEDURE

This study was performed in two phases. First, the L-RBA system was built, calibrated, and then used to observe the vibration of a production read/write head. The L-RBA system was also used to examine the vibration of experimental head designs that were constructed in an attempt to reduce the high-frequency vibration amplitudes. The L-RBA system was used to examine the feasibility of a Reflected Beam Analyzer system. The L-RBA system proved to be a success; thus the A-RBA system, the second phase of the study, was developed to simultaneously obtain data for pitch rotation, roll rotation, and vertical translation. This chapter will describe the use of these systems in examination of the motion of the read/write heads.

Production Head and Experimental Head Designs

The first studies were conducted in an attempt to obtain base data on the amplitude and frequency of vibration in a production read/write head. The production head was analyzed for pitch and roll rotations in the frequency domain using the L-RBA system. Once the base data were obtained, attempts were made to alter the production head design in order to reduce the vibrational amplitudes. These alterations consisted of addition of either a stiffening or damping material to the gimbal structure.

The gimbal structure and stylus of a production head are represented in Figure 19.

The first attempt at reducing the amplitude of vibration consisted of the addition of a 0.03-inch thick ring of a graphite-epoxy material to the gimbal as shown in Figure 20. The graphite-epoxy ring was adhered to the gimbal with an epoxy adhesive. This alteration was designated as Advanced Design Two (AD-2). The addition of the ring effectively stiffens the gimbal and should also create some constrained-layer damping due to the presence of the epoxy adhesive.

A second gimbal alteration, named AD-3, consisted of adding to a production head a ring of vibration damping material that has the same dimensions as the ring used in AD-2. The damping material chosen for this application is LD-400 which is manufactured by United McGill Corporation. LD-400 was determined to have a loss factor of 0.222 at 20 degrees Celsius and 1000 Hz [17]. LD-400 is rather flexible and should add very little stiffness to the gimbal frame but should provide some additional damping effects.

A third design, which shall be called AD-4, incorporated a 0.03-inch thick frame of LD-400 which was attached to a production head gimbal structure as shown in Figure 21. In the design the LD-400 extended over the gimbal arms in an attempt to dampen the entire gimbal structure.

Analyses Using the L-RBA System

The disk drive was placed in the L-RBA system as shown in Figure 22. When the drive is placed in this manner, the L-RBA system can be used to examine pitch rotation and vertical translation of the stylus. To examine

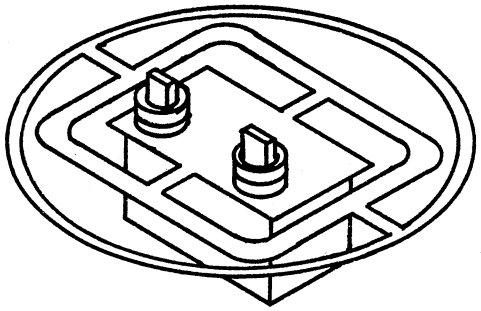

Figure 19. Gimbal System and Stylus of a Production Read/Write Head

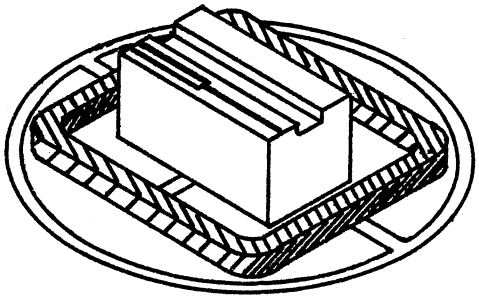

Figure 20. Experimental Design AD-2, Graphite-Epoxy Ring Adhered to Gimbal Structure

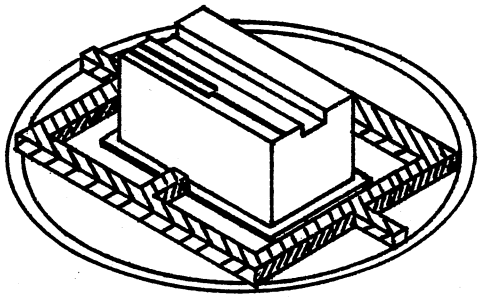

Figure 21. Experimental Design AD-4, LD-400 Damping Material Adhered to Gimbal Structure

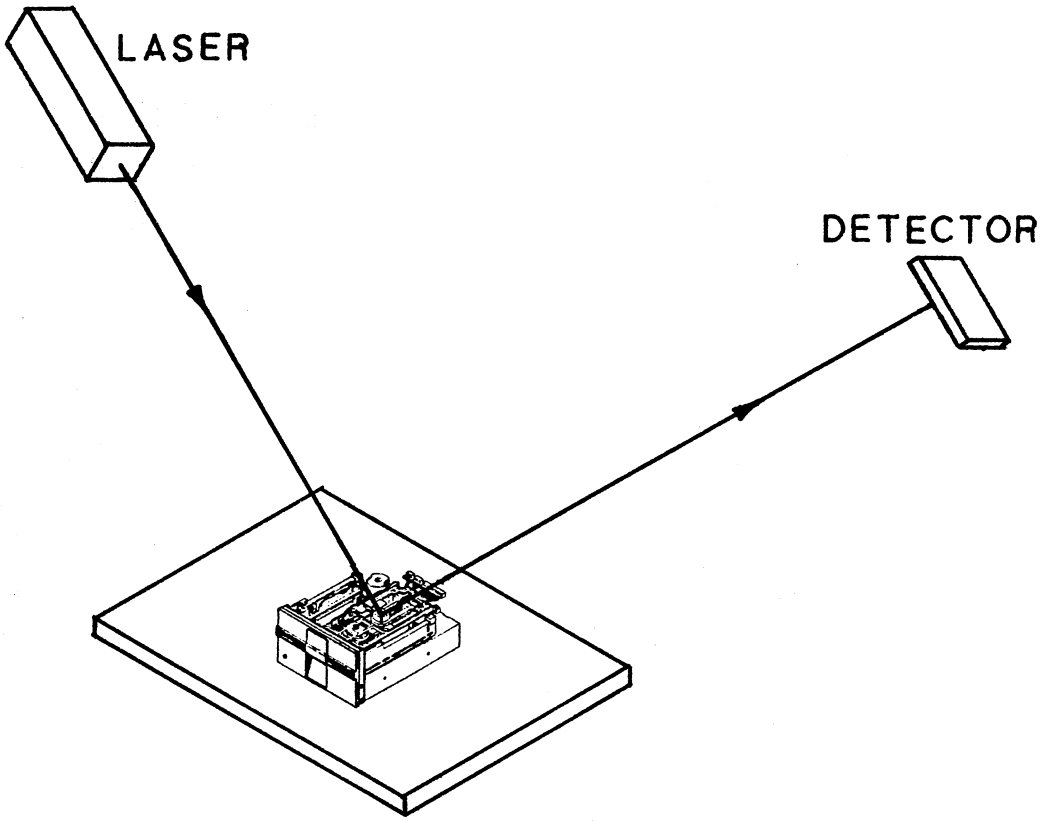

Figure 22. Disk Drive Positioned in the L-RBA System

roll rotation as well as vertical translation, the disk drive must be rotated 90 degrees inside the L-RBA system.

The disk drive was powered by a variable voltage power supply which allowed for continuous drive speed adjustment. A photodiode was placed in the drive to sense the index hole in the disk. The average drive speed could then be determined from the period of the pulses produced as the index hole passed over the photodiode.

For the studies performed with the L-RBA system, the distance R was set at 42.25 inches and the incident angle was set at 45 degrees (see Equation (2.5)). Using these parameters, the system is sensitive to both rotation and vertical translation. The sensitivity of the UDT LSC-5D linear lateral-effect photodiode used in conjunction with a UDT 301-DIV amplifier is 71 volts per inch of beam displacement at its face.

The L-RBA system was used only for analysis in the frequency domain. Signals were obtained in the time domain but these were used for qualitative inspections only. The output signal from the 301-DIV amplifier was examined using a Spectral Dynamics model SD-345 real-time analyzer. The SD-345 converts the analog input signal to discrete digital values with a 12-bit A/D converter which is scaled over the voltage range indicated in the data trace. Output plots of data stored in the SD-345 are generated using a composite video printer. The SD-345 uses a Fast Fourier Transform algorithm to produce the frequency spectrum. A Hanning window weighting function was used to condition the intput signal. Most data were taken over the 0 to 5 KHz range; however, some traces were obtained in other frequency ranges. The SD-345 obtains a 1024 point data record which is sampled at a rate which is 2.56 times the maximum frequency of the selected spectral window. For data taken in the 0 to 5 KHz range,

the total time elapsed in the data trace is 0.08 seconds. This time corresponds to about four-tenths of a rotation of the disk if the disk is rotating at the nominal drive speed of 300 revolutions per minute. The frequency spectra that are shown in the experimental results of the next chapter are linear spectrum averages. The number of samples that were averaged for the given trace is indicated in the lower right-hand corner of the spectrum plot.

The frequency spectrum of the resulting data was inspected for peaks which were well above the noise floor. Data were examined for both pitch and roll rotation directions. Since the L-RBA system is sensitive to vertical translation as well as rotations, the frequency spectrum should also contain some terms which are related to translation; however, if this is the case, then the frequency content associated with vertical translation should be evident in both the frequency spectra obtained for pitch and roll signals. The peaks that are distinct for either the pitch or roll direction can be analyzed and a rotation amplitude determined by using Equation (2.7). The term $\Delta_{\phi t}$ of Equation (2.7) is found by dividing the output voltage amplitude associated with the frequency component of interest by the sensitivity of the linear lateral-effect photodiode.

Analyses Using the A-RBA System

The A-RBA system was configured as shown in Figure 23. The pitch rotation and vertical translation of the stylus can be calculated using the output signal from the y-axis of detectors one and two. The roll rotations can be calculated from the output of the x-axis of either detector. Comparison of roll rotations calculated from both detectors will reveal the expected accuracy of the calculated roll values.

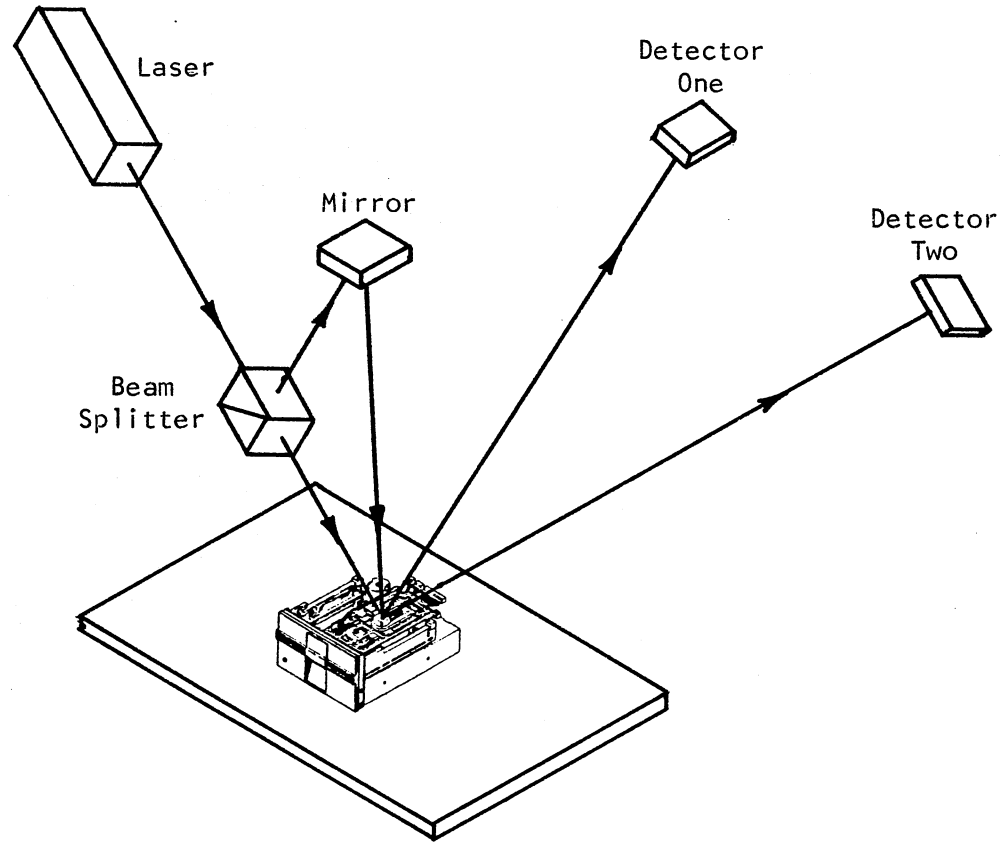

Figure 23. Disk Drive Positioned in the A-RBA System

The drive speed was controlled and monitored in the same manner as that mentioned for the L-RBA system. The distance R from the mirror atop the stylus to the face of each detector was set at 35 inches. Detector one was set at an angle ψ of 68.5 degrees and detector two set at 48.5 degrees. The sensitivity of both detectors in both x- and y-directions was found in the calibration procedure to be 71 volts/inch.

A schematic of the instrumentation used with the A-RBA system is shown in Figure 24. The output of the four 301-DIV amplifiers was analyzed using a DATA 6000 Waveform Analyzer which is manufactured by the Data Precision Division of Analogic Corporation. The DATA 6000 is a four-channel analyzer capable of performing a multitude of mathematical manipulations on the stored data sets. The functions most used in this study are the FFT and the cross-correlation.

The DATA 6000 can acquire four channels of data simultaneously. This is a required feature which makes it possible to separate output signals generated by pitch rotation and vertical translation simultaneously with the roll rotations. Using all four channels, the DATA 6000 has a maximum single channel sampling frequency of 25 KHz. The four input connections of the DATA 6000 lead to four sample and hold circuits which are multiplexed in turn to a 14-bit A/D converter which operates at a maximum sampling rate of 100 KHz. The A/D converter can be set for a full scale input range of either 0.5, 5.0, or 50 volts.

The A-RBA system was primarily used to examine data in the time domain. Using the four channels of data obtained in the time domain, Equations (2.23), (2.24), and (2.25) can be solved for each point in time. If the DATA 6000 inputs are set for AC coupling, then the displacement values calculated using Equations (2.23) through (2.25) will be the

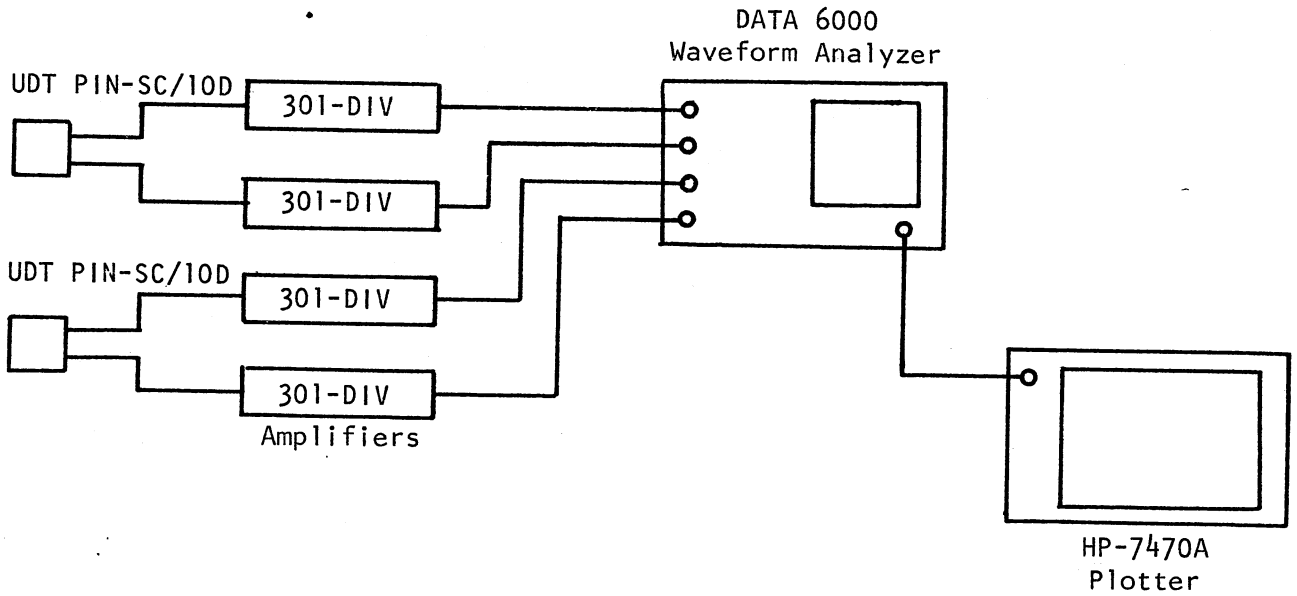

Figure 24. Schematic of A-RBA System Instrumentation

displacement from the steady-state operating point of the stylus. With the DATA 6000 inputs set for DC coupling, the displacements found are absolute and the steady-state operating position of the stylus, referenced to the position at startup, can be determined. Note that it requires that the data traces must contain the initial output voltages at the time of drive startup so that the remaining data points can be referenced from the startup values.

A study in the frequency domain was conducted to determine if there were vibrational modes present in the production head which occurred in a direction which was a combination of pitch and roll rotation. To determine the modes which possibly contained both pitch and roll rotation, the signals obtained from the x- and y-axis of either detector were cross-correlated and the results of the cross-correlation were analyzed by taking its FFT. The spectrum obtained by this method is called the cross-spectral density [18]. Peaks in the cross-spectrum indicate the frequencies which are common to both pitch and roll rotation signals.

In theory, Equations (2.23), (2.24), and (2.25) could be solved inside the DATA 6000 and the resulting separated data sets could be analyzed in the frequency domain by taking their FFT. This would result in three frequency spectra which would represent pitch rotation, roll rotation, and vertical translation. It appears that this process should work; however, an attempt at this procedure revealed that when the data sets were subtracted inside the DATA 6000, discontinuities were evident in the resulting data sets. This resulted in a high noise floor in the frequency spectrum when a FFT was performed on the data set. The noise floor was of sufficient amplitude to render the frequency spectrum useless for examination of low-amplitude values.

CHAPTER IV

EXPERIMENTAL RESULTS

Several factors combine to determine the frequency and amplitude of stylus vibrations. The forcing function which causes stylus vibration consists of both a low-frequency part which is nearly periodic and a high-frequency part which is random. The low frequency portion of the forcing function is associated with motion of the flexible disk. The high-frequency excitation is associated with a friction-type random forcing function which produces a broad-band excitation of some finite bandwidth.

The experimental results that are presented in this chapter are subject to random variation of vibrational amplitude; thus the amplitude data that are presented cannot be assumed to consist of fixed values common to duplicate test situations. The amplitude of the high-frequency vibrational modes can easily vary from one set of tests to another by a factor of 4 or higher. This variation is due to the random characteristics of the high-frequency forcing function. The results reveal dominant high-frequency vibrational modes for both pitch and roll rotations; however, it will be shown that "identical" read/write heads will exhibit sometimes greatly different signatures in the frequency domain when subjected to the same conditions.

Both the L-RBA and A-RBA systems proved to be useful as analysis tools. The results obtained in the frequency domain using the A-RBA system supports the findings of the L-RBA system but has the distinct

advantage of examining pitch rotation, roll rotation, and vertical translation simultaneously. The L-RBA system was used to examine both pitch and roll rotations but not simultaneously. Due to the randomness of the vibrational amplitudes, it cannot be assumed that test situations can be repeated identically as would be required for direct comparison of pitch and roll values obtained with the L-RBA system.

The studies performed in the time domain using the A-RBA system reveals the displacements of the stylus in time and also reveals much about the interaction of the gimbal system with the flexible disk. Use of the A-RBA system allows for examination of the steady-state rotational position of the stylus. Also, examination of data taken upon shutoff of the disk drive proved to allow for comparison of the overall head system damping of the production head and AD-4.

Results Using the L-RBA System

The L-RBA system was used to examine a production head as well as experimental designs AD-2, AD-3, and AD-4 in the frequency domain. The tests were performed with the same diskette while drive rotational speed and track position were variable factors.

Before presenting the results and some quantitative data, the author would like to reiterate the concept that supposedly identical heads will not reveal identical responses when subjected to like test conditions. Figure 25 contains the frequency spectra for two production heads which appear to be identical from a visual inspection. These tests were performed at 300 RPM in the outside track position. It can be seen that the responses are similar in some frequency ranges while a different response is evident in others. This variation in frequency response can

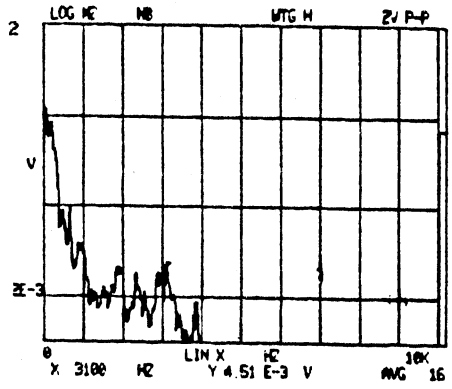

Pitch

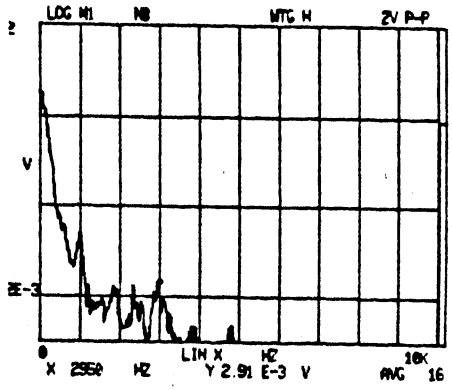

Roll

Head No. 1

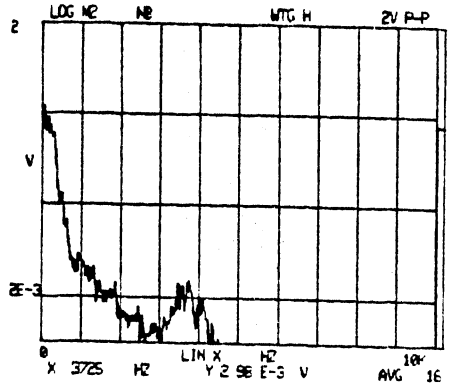

Pitch

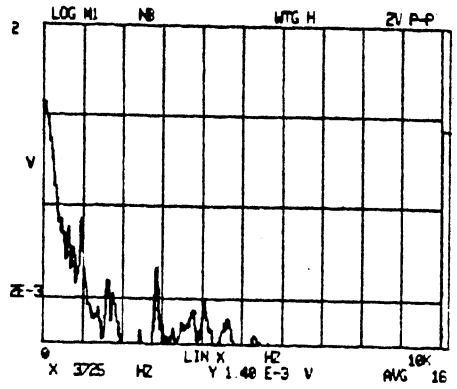

Roll

Head No. 2

Figure 25. Pitch and Roll Spectra of Two Production Heads

be caused by a number of factors such as differences in the chamfer of the stylus and minor variations in the stiffness, mass, or boundary conditions of the stylus/gimbal system. Because of the relatively small size of the stylus/gimbal system, the eigenvalues and eigenvectors are rather sensitive to small variations in the above mentioned parameters.

Frequency Response of Production Head

A production head was examined in the frequency domain using the L-RBA system. A typical plot of the frequency spectrum is shown in Figure 26. These data were taken at the outside track position and at 300 RPM which is the factory-set drive speed. The dominant peak in the high-frequency portion of the pitch rotation spectrum occurs at 3712 Hz with a zero-to-peak rotational amplitude of 60.3(-6) degrees. The dominant high-frequency roll motion occurs at 1612 Hz with an amplitude of 10.7 (-6) degrees.

Inspection of the frequency spectra of Figure 26 reveals that low-frequency motions are two orders of magnitude larger than the high-frequency components. The low-frequency components must correspond to motions that occur as the stylus follows waves in the flexible disk. The high-frequency modes consist of a relative motion between the stylus and disk surfaces and thus are at least partially responsible for excessive media wear. Note that the high-frequency broad-band excitation is not as evident in the roll direction as it is in the pitch direction. This is the expected result as the friction-type forcing function acts essentially in the pitch direction. Tables X and XI contain data taken for the dominant high-frequency mode in the pitch and roll directions, respectively. It is evident from these data that some frequency shift

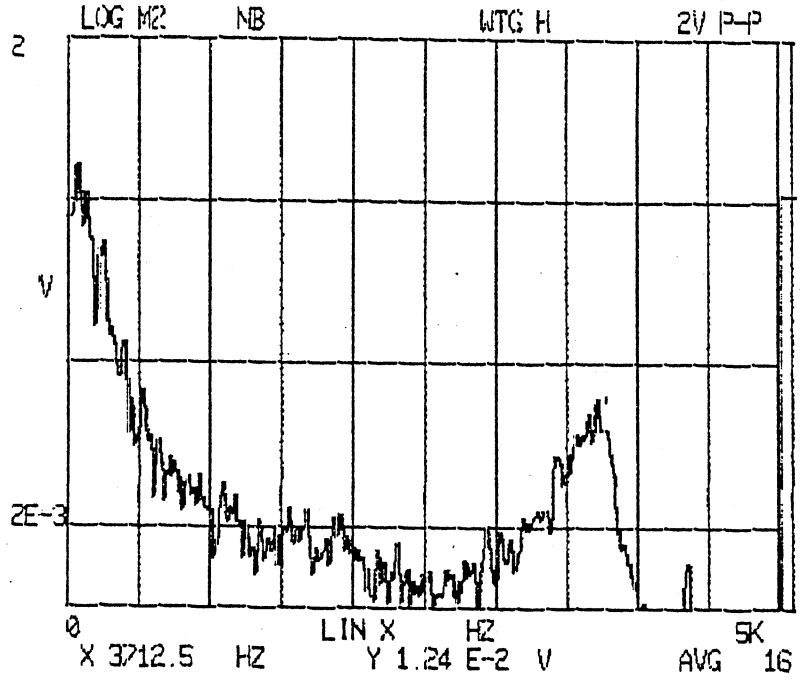

Pitch Spectrum

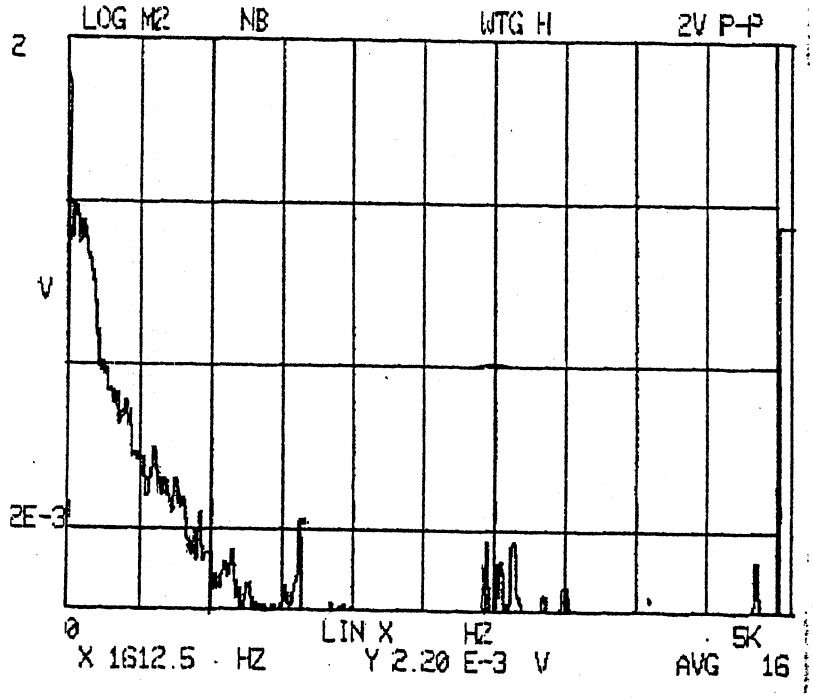

Roll Spectrum

Figure 26. Pitch and Roll Spectra for Production Head, Drive Speed 300 RPM, Outside Radial Track

TABLE X

DOMINANT HIGH-FREQUENCY PITCH MODE OF THE PRODUCTION HEAD AT 300 RPM DRIVE SPEED IN THE OUTSIDE, MIDDLE, AND INSIDE RADIAL TRACK POSITIONS

Radial Track Position	Mode Frequency (Hz)	Amplitude (Degrees)
Outside	3712	60.30(-6)
Middle	3500	26.90(-6)
Inside	3425	29.00(-6)

TABLE XI

DOMINANT HIGH-FREQUENCY ROLL MODE OF THE PRODUCTION HEAD AT 300 RPM DRIVE SPEED IN THE OUTSIDE, MIDDLE, AND INSIDE RADIAL TRACK POSITIONS

Radial Track Position	Mode Frequency (Hz)	Amplitude (Degrees)
Outside	1612	10.70(-6)
Middle	1612	7.14(-6)
Inside	1612	14.50(-6)

occurs in the pitch modes when radial track position is changed. This is possibly due to an increased disk stiffness and enforced buckling deformation in the disk as a result of hub/disk interference that are present at the inside track position. This would result in different boundary conditions as well as a change in the forcing functions. From Figure 26 it can be seen that the 1612 Hz roll mode has a much narrower bandwidth as compared with the 3712 Hz pitch mode. Also, the roll mode does not exhibit a significant frequency shift when radial track position is changed.

A test was performed to determine the effects of media velocity on the amplitude of a high-frequency pitch mode. This test was performed at the outside radial track position. The pitch mode that was examined occurs near 3550 Hz. The numerical results of this examination are given in Table XII and a plot of these data is shown in Figure 27. It is seen that the vibrational amplitude increases with increasing media velocity. It appears that this mode begins to go somewhat unstable at a media velocity of about 75 inches per second. At 75 inches per second, the mode frequency began to shift upward from the 3550 Hz value typical of all lower media velocities. The frequency had shifted to 3675 Hz at the uppermost test velocity of 110.6 inches per second. The media velocity at the factory-set drive speed of 300 RPM in the outside track position is approximately 69 inches per second; thus when at the outside track the stylus is operating near the unstable or transition range of this 3550 Hz mode.

Frequency Response of Experimental Head Designs

The experimental head designs AD-2, AD-3, and AD-4 were tested to

TABLE XII

AMPLITUDE OF 3550 HZ PITCH MODE
OF THE PRODUCTION HEAD FOR
VARIOUS MEDIA VELOCITIES

Media Velocity (Inches/Second)	Pitch Amplitude (Degrees)
13.8	8.9(-6)
20.7	9.8(-6)
27.7	10.4(-6)
34.6	12.1(-6)
41.5	13.7(-6)
48.4	15.3(-6)
55.3	20.2(-6)
62.2	20.3(-6)
69.1	25.8(-6)
76.0	28.0(-6)
82.9	39.0(-6)
89.9	55.9(-6)
97.8	50.1(-6)
103.7	56.9(-6)
110.6	60.7(-6)

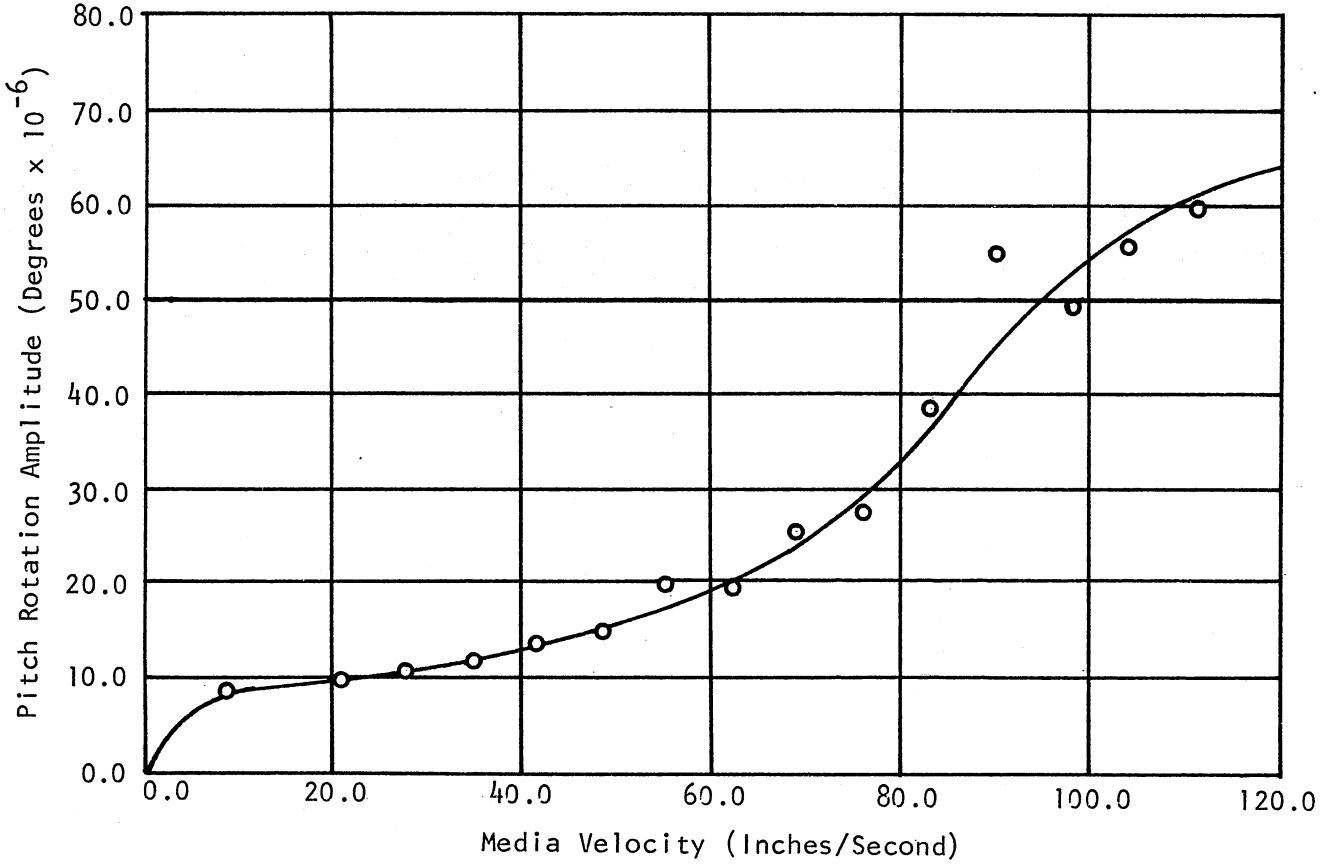

Figure 27. Pitch Rotation Amplitude Versus Media Velocity, 3550 Hz Pitch Mode, Outside Radial Track

determine if the high-frequency vibrational amplitudes could be reduced by the addition of stiffening rings or damping material to the gimbal structure. It is important that any changes made should not greatly change the stiffness of the gimbal system, as such a change could result in unsatisfactory head/disk compliance. It has been shown that the low-frequency stylus motions are of much greater amplitude than those of the high-frequency motions. With this in mind, a design change which reduces the high-frequency vibrations could present new problems, associated with improper compliance, which are more severe than those which they "fixed."

Any alteration of the gimbal structure will undoubtedly change the eigenvalues of the system; thus a direct comparison of frequency components with those of the production head will not be possible. A full series of tests were performed on each of the three designs. Each design was examined for pitch and roll rotations at inside and outside track positions and at various drive rotational speeds.

The results of tests performed on AD-2 are given in Tables XIII and XIV. Figure 28 is the frequency spectra of AD-2 for pitch and roll at the outside track position with the drive speed set at 300 RPM. From comparison of Figures 26 and 28, it can be seen that addition of the graphite epoxy ring did indeed change the eigenvalues of the gimbal system. Comparison of vibrational amplitudes with those of the production head reveals that the maximum amplitudes of the high-frequency pitch modes of AD-2 were reduced by a moderate amount; however, there appears to be a slight increase in the amplitude of the dominant high-frequency roll modes. In view of these findings, AD-2 does not appear to be an improvement

TABLE XIII

AMPLITUDE OF DOMINANT HIGH-FREQUENCY PITCH MODES OF AD-2 FOR OUTSIDE AND INSIDE RADIAL TRACK POSITIONS AND VARIOUS DRIVE SPEEDS

Drive Speed (RPM)	Outside Radial Track		Inside Radial Track	
	Mode Frequency (Hz)		Mode Frequency (Hz)	
	1750	4300	1750	4300
	Amplitude (°)	Amplitude (°)	Amplitude (°)	Amplitude (°)
300.0	19.5(-6)	12.3(-6)	9.4(-6)	10.8(-6)
240.0	14.4(-6)	9.3(-6)	8.8(-6)	9.7(-6)
180.0	10.1(-6)	6.5(-6)	*	*
120.0	5.4(-6)	6.9(-6)	*	*

*Data not obtained for these values.

TABLE XIV

AMPLITUDE OF DOMINANT HIGH-FREQUENCY ROLL MODES OF AD-2 FOR OUTSIDE AND INSIDE RADIAL TRACK POSITIONS AND VARIOUS DRIVE SPEEDS

Drive Speed (RPM)	Outside Radial Track		Inside Radial Track	
	Mode Frequency (Hz)		Mode Frequency (Hz)	
	950	1850	750	1700
	Amplitude (°)	Amplitude (°)	Amplitude (°)	Amplitude (°)
300.0	44.8(-6)	21.4(-6)	38.8(-6)	10.7(-6)
240.0	24.9(-6)	14.4(-6)	86.5(-6)	10.2(-6)
180.0	13.5(-6)	9.6(-6)	*	*
120.0	13.5(-6)	4.9(-6)	*	*

*Data not obtained for these values.

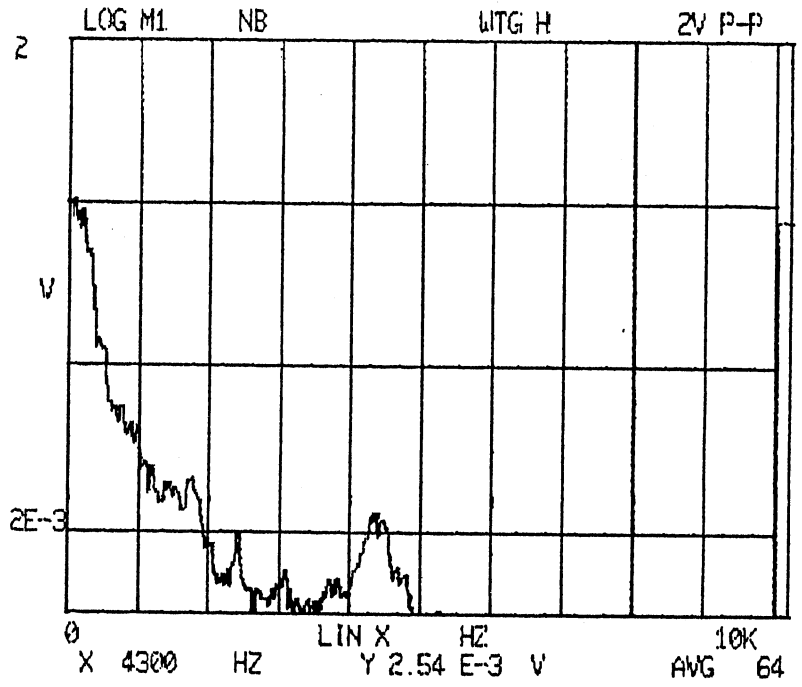

Pitch Spectrum

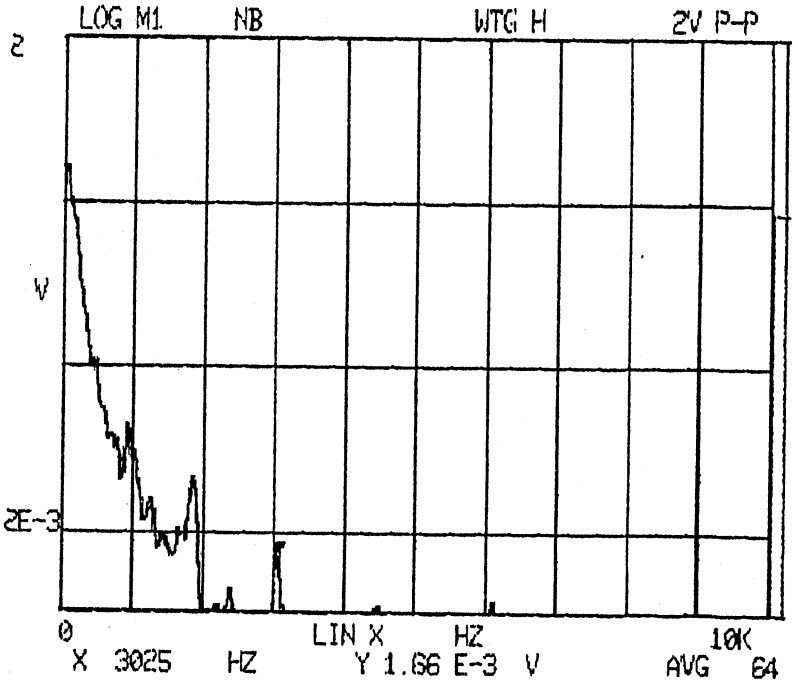

Roll Spectrum

Figure 28. Pitch and Roll Spectra for AD-2, Drive Speed 300 RPM, Outside Radial Track

over the production head; therefore, this design need not be examined further.

Figure 29 contains the spectral plots obtained from design AD-3 at the outside track position and at a drive speed of 300 RPM. The data for all tests performed on AD-3 are presented in Tables XV and XVI. Again, comparison with the data from tests on the production head reveal that, like design AD-2, AD-3 resulted in reduced pitch rotation amplitudes but did not reduce the amplitude of the roll components. Also note that the addition of the LD-400 damping material did not affect the high-frequency system eigenvalues to the extent that AD-2 did. This is expected since the LD-400 should not greatly change the gimbal stiffness or at least not to the degree that was evident from the addition of the graphite-epoxy material of design AD-2. Design AD-3 did not prove to be successful in reducing the high-frequency vibrations; thus further investigations were not pursued.

The final experimental design, AD-4, proved to dramatically reduce the high-frequency stylus vibrations. Like experimental design AD-3, LD-400 was used as the damping material, but in design AD-4 the LD-400 covered the gimbal arms in addition to the portion of the gimbal that was covered in AD-3. The frequency spectra for pitch and roll rotations of design AD-4 are shown in Figure 30. Inspection of Figure 30 reveals that at frequencies above 1000 Hz, all peaks but one have amplitudes well below two millivolts. A two-millivolt voltage corresponds to about a 9.0 (-6) degree rotation amplitude. Thus, there is a great overall reduction in high-frequency pitch vibrations. No distinct high-frequency pitch modes were evident in the tests that were performed; therefore, no tabular data are presented for the pitch vibrations. The data obtained

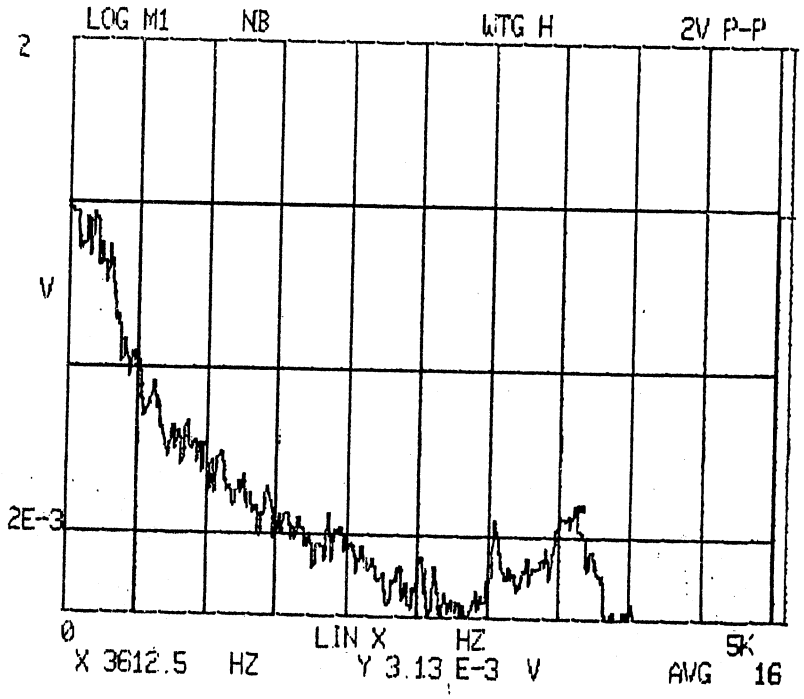

Pitch Spectrum

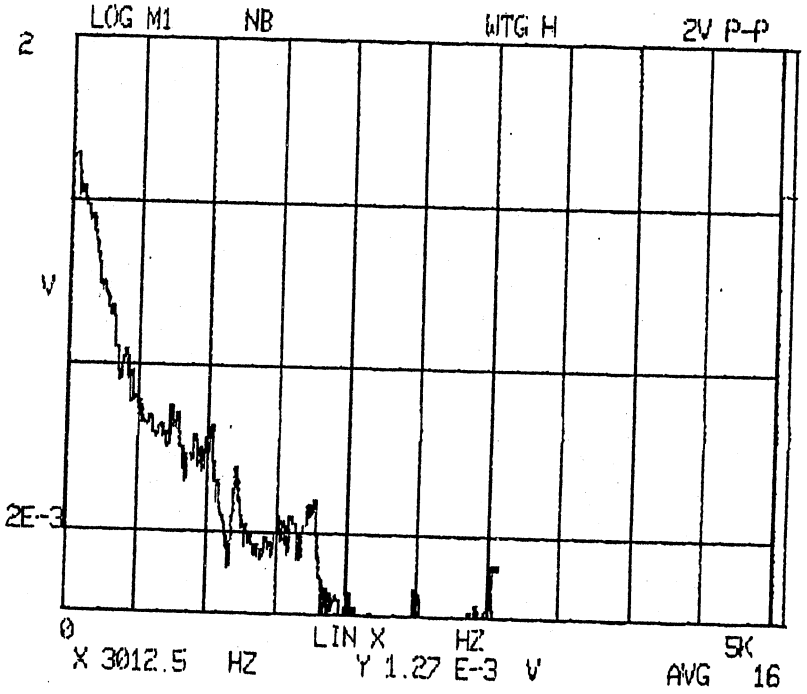

Roll Spectrum

Figure 29. Pitch and Roll Spectra for AD-3, Drive Speed 300 RPM, Outside Radial Track

TABLE XV

AMPLITUDE OF DOMINANT HIGH-FREQUENCY PITCH MODES OF AD-3 FOR OUTSIDE AND INSIDE RADIAL TRACK POSITIONS AND VARIOUS DRIVE SPEEDS

Drive Speed (RPM)	Outside Radial Track		Inside Radial Track	
	Mode Frequency (Hz)		Mode Frequency (Hz)	
	3050	3625	3050	3626
	Amplitude (°)	Amplitude (°)	Amplitude (°)	Amplitude (°)
360.0	99.6(-6)	15.4(-6)	12.0(-6)	15.1(-6)
300.0	11.9(-6)	15.2(-6)	7.1(-6)	12.3(-6)
240.0	6.5(-6)	10.5(-6)	4.8(-6)	7.6(-6)
180.0	6.0(-6)	10.2(-6)	*	6.0(-6)
120.0	3.4(-6)	9.1(-6)	3.0(-6)	4.1(-6)
72.0	*	5.8(-6)	2.6(-6)	4.4(-6)

*Data not obtained for these values.

TABLE XVI

AMPLITUDE OF TWO HIGH-FREQUENCY ROLL MODES OF AD-3
FOR OUTSIDE AND INSIDE RADIAL TRACK POSITIONS
AND DRIVE SPEEDS OF 300 AND 240 RPM

Drive Speed (RPM)	Outside Radial Track		Inside Radial Track	
	Mode Frequency (Hz)		Mode Frequency (Hz)	
	1200	1725	1200	1725
	Amplitude (°)	Amplitude (°)	Amplitude (°)	Amplitude (°)
300.0	24.1(-6)	15.6(-6)	*	7.34(-6)
240.0	16.5(-6)	13.1(-6)	6.17(-6)	8.41(-6)

*Data not obtained for this value.

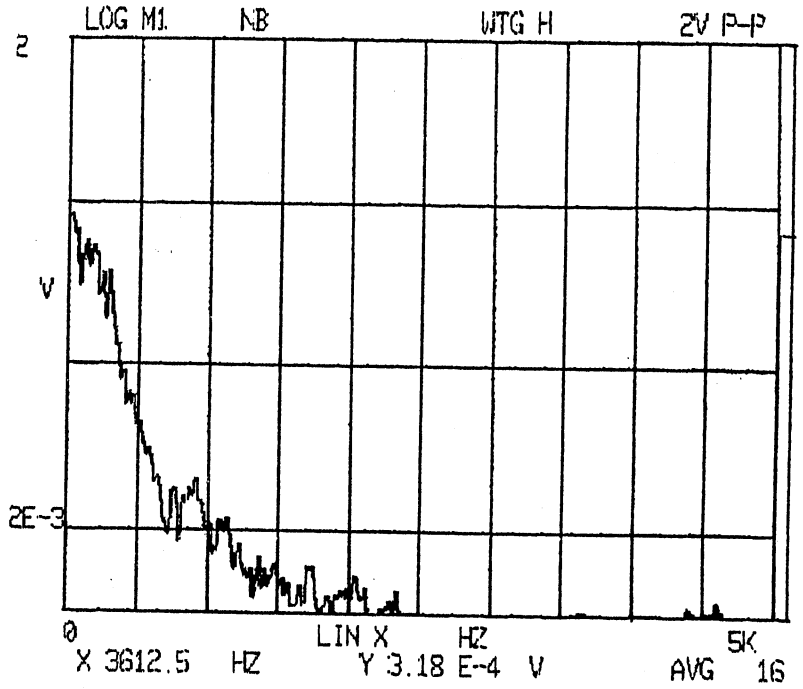

Pitch Spectrum

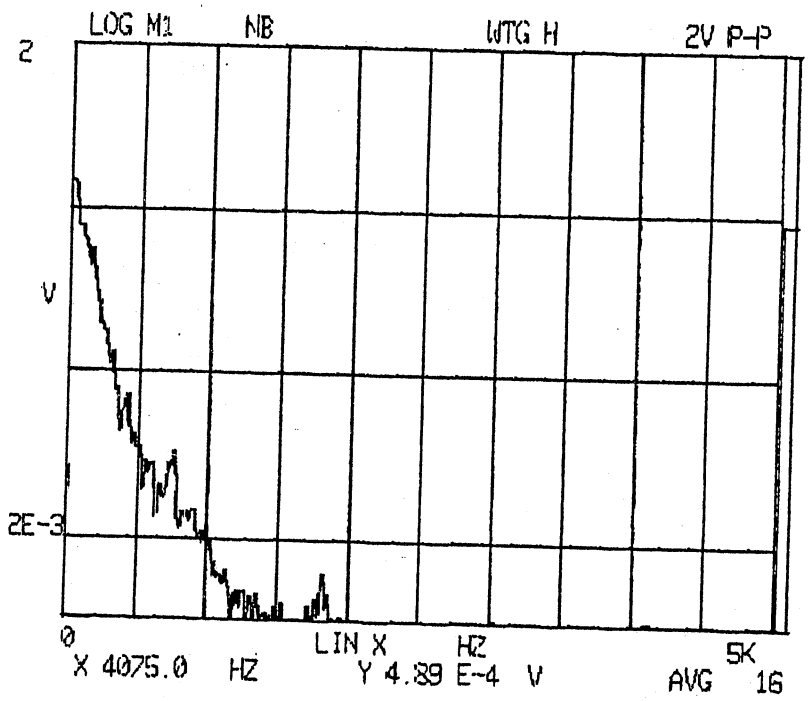

Roll Spectrum

Figure 30. Pitch and Roll Spectra for AD-4, Drive Speed 300 RPM, Outside Radial Track

for the 1825 Hz roll mode of AD-4 are presented in Table XVII. These roll amplitudes are comparable to the 1612 Hz mode of the production head but are slightly smaller. In view of these results, design AD-4 represents a possible means by which high-frequency stylus vibrations could be reduced, thus resulting in extended head and media life. The addition of the damping media does not significantly stiffen the gimbal structure. From the manufacturing standpoint, consideration of a damping material which is supplied in a liquid form may prove to be more suitable and possibly more effective.

Results Using the A-RBA System

The A-RBA system was primarily used for studies in the time domain. In a first test, the A-RBA system was used to determine simultaneously the pitch, roll, and vertical translation displacements of the production head at steady-state operating conditions. In a second study, the production head and experimental design AD-4 were examined to determine their steady-state rotational offset position. A third study provided a means by which the overall damping characteristics of the production head and AD-4 could be compared. In a final study, the production head was examined in the frequency domain to determine the relation between pitch and roll signals.

Displacements of the Production Head in the Time Domain

A production head was examined using the A-RBA system to determine the displacements associated with pitch, roll, and vertical translation. This analysis was performed at a drive speed of 300 RPM with the head

TABLE XVII

AMPLITUDE OF 1825 HZ ROLL MODE OF AD-4 FOR OUTSIDE AND INSIDE RADIAL TRACK POSITIONS AND VARIOUS DRIVE SPEEDS

Drive Speed (RPM)	Outside Track Amplitude (Degrees)	Inside Track Amplitude (Degress)
300.0	5.5(-6)	3.7(-6)
240.0	4.3(-6)	2.7(-6)
180.0	2.7(-6)	*

*Data not obtained for this value.

positioned at the outside track position. The results of this test will produce the displacements at discrete points in time. The displacements that are found will be essentially due to low-frequency motion of the stylus as it follows the disk surface. Since the high-frequency movements are of such small amplitude, their contribution to the overall displacements will be negligible.

The four time traces obtained in this test are contained in Figures 31 and 32. Figure 31 contains the two pitch signals from the y-axis of the array detectors while Figure 32 contains the two roll signals from the x-axis of the array detectors. The voltage traces are essentially periodic with a period of approximately 0.2 seconds which would correspond to the time required for one rotation of the flexible disk. As expected, the two pitch signals appear to have exactly the same shape and the same is true for the two roll signals; however, the pitch and roll signals are significantly different. This fact indicates that the pitch and roll signals of the A-RBA system are well separated.

Numerical voltage data were obtained from a portion of the traces of Figures 31 and 32. These voltage data were analyzed for pitch, roll, and vertical translation at discrete points in time by solving Equations (2.23), (2.24), and (2.25) through use of the computer program listed in the Appendix. A portion of the calculated displacements obtained from this procedure are listed in Table XVIII. The maximum displacements found in the time interval under investigation are presented in Table XIX.

The maximum pitch and roll displacements are seen to be of about the same magnitude. Again, it is important to realize that these angular displacements, for the most part, correspond to the motion of the stylus

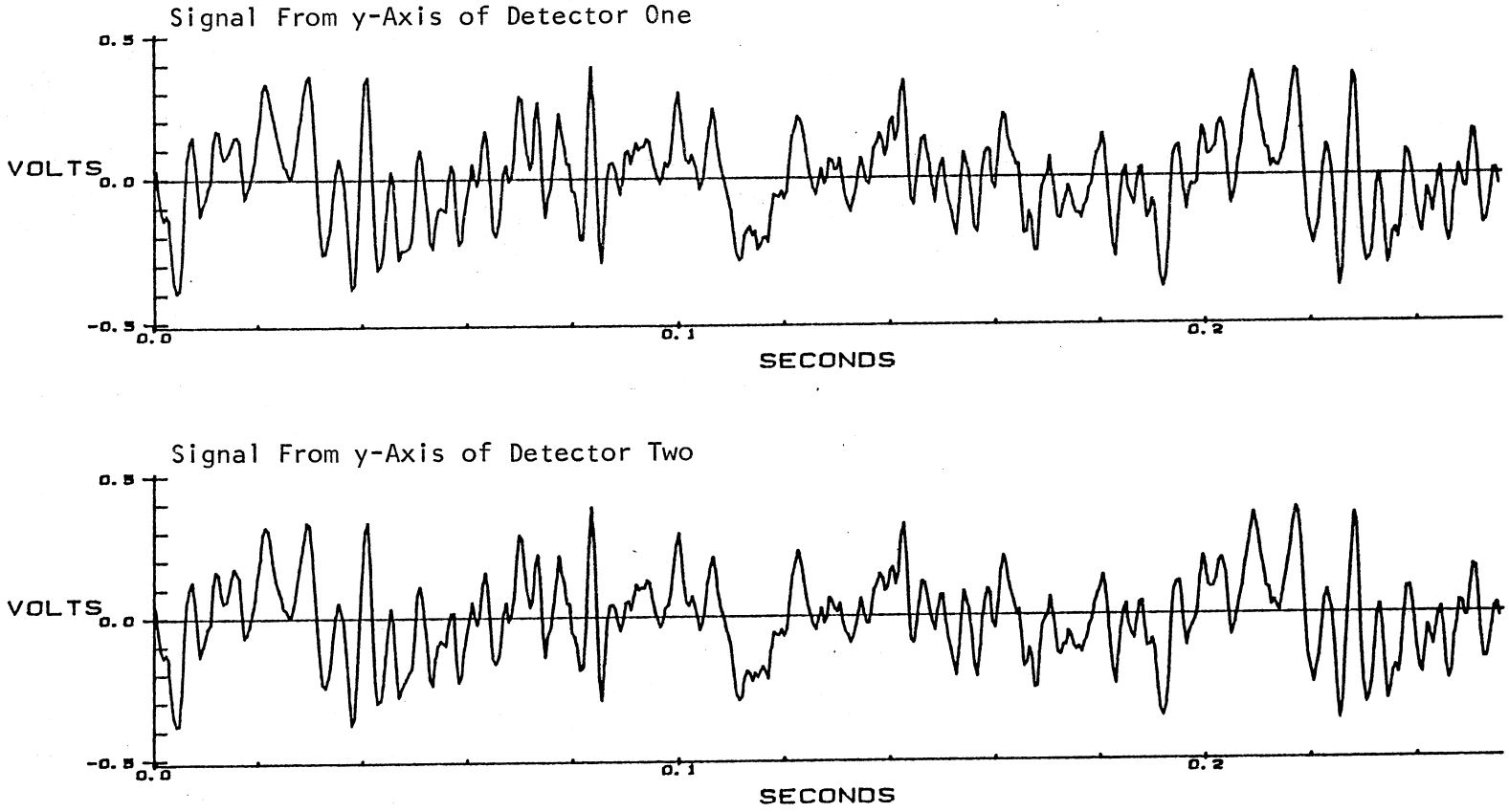

Figure 31. Steady-State Response of Production Head, Signals Due to Pitch Rotation and Vertical Translation

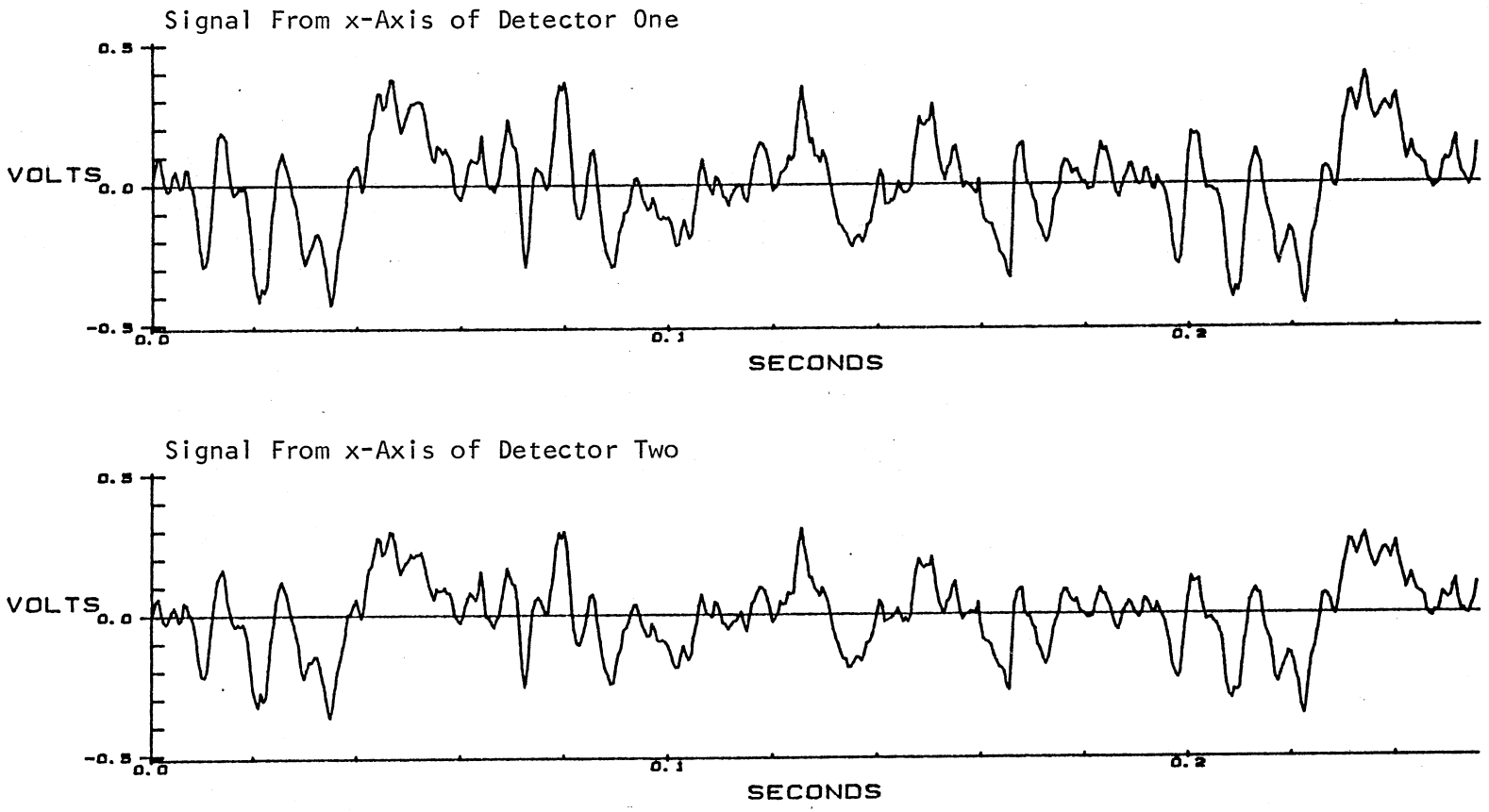

Figure 32. Steady-State Response of Production Head, Signals Due to Roll Rotation

TABLE XVIII

DISPLACEMENT AMPLITUDES OF THE PRODUCTION HEAD IN STEADY-STATE OPERATION

DATA Time (Ms)	Pitch Rotation (Degrees)	Vertical Translation (Inches)	Roll Rotation Detector One (Degrees)	Roll Rotation Detector Two (Degrees)
0.0	0.190E-03	0.349E-03	0.200E-03	0.673E-05
10.0	-0.699E-03	-0.106E-03	-0.362E-02	-0.333E-02
20.0	0.194E-02	-0.227E-03	-0.397E-02	-0.405E-02
30.0	0.465E-02	-0.800E-03	-0.349E-02	-0.346E-02
40.0	0.241E-02	-0.415E-03	0.896E-03	0.914E-03
50.0	-0.120E-02	0.334E-03	0.341E-02	0.303E-02
60.0	-0.749E-03	0.120E-03	-0.614E-03	-0.389E-03
70.0	0.325E-02	0.114E-03	0.177E-02	0.177E-02
80.0	-0.314E-03	-0.315E-03	0.455E-02	0.459E-02
90.0	0.163E-02	-0.959E-03	-0.286E-02	-0.274E-02
100.0	0.350E-02	-0.878E-04	-0.140E-02	-0.166E-02
110.0	-0.134E-02	0.402E-04	0.852E-05	0.206E-03
120.0	-0.876E-03	0.505E-04	-0.240E-03	-0.408E-03
130.0	0.531E-03	-0.343E-03	0.119E-02	0.117E-02
140.0	0.268E-02	-0.777E-03	0.156E-03	0.112E-03
150.0	0.556E-03	0.250E-03	0.281E-02	0.265E-02
160.0	-0.407E-03	-0.120E-03	-0.898E-03	-0.565E-03
170.0	0.156E-03	-0.174E-03	-0.595E-03	-0.642E-03
180.0	0.111E-02	-0.357E-04	0.128E-03	0.452E-04
190.0	-0.862E-03	-0.164E-03	0.149E-03	0.962E-06
200.0	0.116E-02	0.684E-03	0.138E-02	0.942E-03
210.0	0.331E-02	-0.284E-03	-0.433E-02	-0.410E-02
220.0	-0.242E-02	0.684E-04	-0.205E-02	-0.219E-02
230.0	-0.279E-02	-0.137E-03	0.287E-02	0.273E-02
240.0	-0.117E-02	-0.327E-03	0.391E-02	0.395E-02
250.0	0.452E-03	0.528E-03	0.976E-03	0.796E-03

TABLE XIX

MAXIMUM DISPLACEMENT AMPLITUDES OF THE PRODUCTION HEAD

Maximum Pitch Rotation	4.60(-3) Degrees
Maximum Roll Rotation	5.30(-3) Degrees
Maximum Vertical Translation	0.96(-3) Inches

as it traverses waves in the flexible disk. Inspection of the roll rotations calculated from detectors one and two reveals that at many times there is significant discrepancy in the two values. A point-by-point analysis of roll rotation accuracy yields little information about the overall expected accuracy. Instead of a point-by-point analysis, the author examined the difference in the RMS values of the set of calculated roll rotations. The RMS difference of the two sets of roll rotation values was found to be 0.00152 degrees. This can be compared to the RMS value of the roll rotations found using detector one which is 0.0158 degrees. Comparison of these RMS values indicates there is a 9.6 percent difference in the RMS values of the two roll data sets.

A similar analysis was performed to examine the validity of the values found for vertical translation. This analysis was performed using the raw voltage data rather than the calculated displacements. The RMS difference in the pitch voltages was found to be 0.0159 volts as compared with a RMS voltage value from the y-axis of detector one which is 0.153 volts. This indicates a RMS difference of 10.4 percent which is much the same as the error associated with the roll signals. Since the translation values are calculated from the difference of the two pitch signals, and this difference represents only about 10 percent of the total amplitude, the accuracy and validity of the translational values are questioned. Although there is some question concerning the accuracy of the vertical translation values, it is likely that the true translation values are no greater than those that were calculated.

The error that is evident from inspection of the calculated roll values is somewhat larger than expected. The true cause of the large error is uncertain; however, there are several factors which alone, or

in combination, could be partially responsible. The factor which is most important is the sensitivity values calculated for the photodiodes. If the sensitivities of the photodiodes are significantly different (which was not evident upon calibration), then such errors would be certain. A second possible cause of the error is the difference in the shape and intensity of the beams which strike the detectors. In theory, the lateral-effect photodiodes, when used in conjunction with the proper type of amplifier (i.e., UDT 301-DIV), have output responses which are independent of beam shape and intensity; however, in actual use this may not be a totally correct assumption. A third possibility is a difference in the gain of the amplifiers; however, this factor should have been eliminated through the calibration procedure as the amplifiers were dedicated to use on a certain axis of a certain detector in both calibration and test data acquisition. A fourth possibility is the effect of displacements in directions assumed to be restrained (i.e., yaw rotation and translation in the x- and y-directions). This is possible but not probable, as this effect would be evident in each detector and thus the undesired motion would have to be of significant magnitude to represent a 10 percent difference in the roll signals. In view of all of the above mentioned factors, the author believes that the sensitivities and differences in reflected beam shape and intensity are the major contributors to the apparent error.

Steady-State Rotational Offset of the Production Head and AD-4

This study was performed to examine the stylus motion of the production head and AD-4 as they are in transition from startup to steady-state

drive conditions. The data traces used in this study were taken with the DATA 6000 Waveform Analyzer. The DATA 6000, with input channels coupled for DC signals, was set to trigger data acquisition when the motor of the disk drive was switched on; thus all stylus motions could be referenced from the rest position. These analyses are performed using only one of the two detectors of the A-RBA system. The use of only one detector requires the assumption that the signal from the y-axis of the array detector is due essentially to pitch rotation. The results of the previous section suggest that this assumption will result in errors of less than 10 percent.

Figures 33 and 34 are the voltage traces obtained from startup of the production head and correspond to pitch and roll signals, respectively. Figures 35 and 36 are the corresponding data for AD-4. Figures 33 through 36 have dashed lines which indicate the steady-state operating envelope of the styli. Another dashed line is drawn at the mean value of the operating envelope. From the voltages associated with the position of these dashed lines, the steady-state offset and maximum steady-state vibration amplitude can be calculated. These values, calculated for the production head and AD-4, are presented in Table XX. Note that the sign convention of the calculated offset positions is consistent with the coordinate system shown in Figure 4.

It can be seen that the steady-state operating point of the stylus does not coincide with the rest position. It might be expected that the media forces the leading edge of the stylus downward due to the frictional forces between the stylus and disk; however, these data indicate that, for both heads, the styli raise upward at the leading edge (pitch rotation). The most likely explanation of these phenomena is the

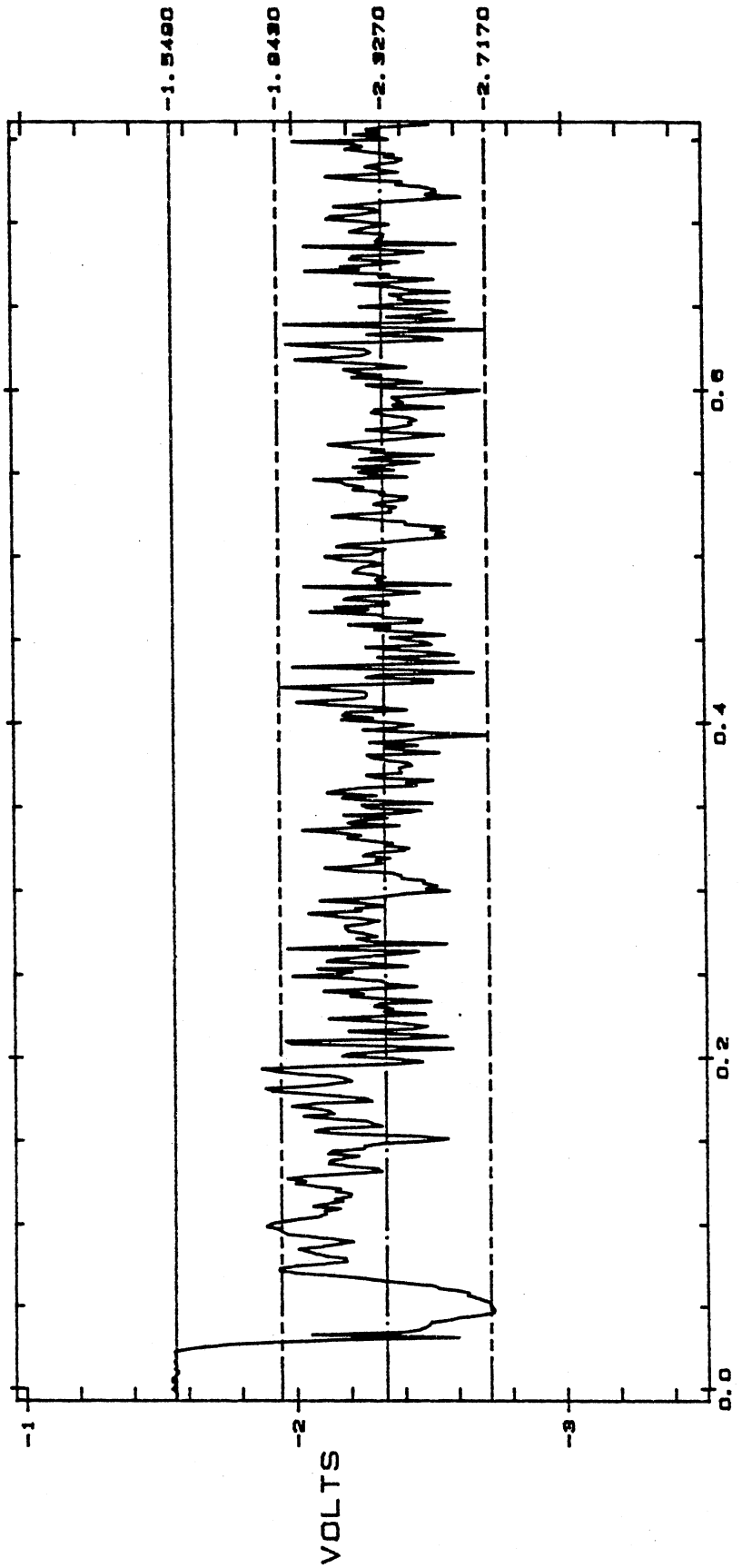

Figure 33. Production Head Response at Startup, Pitch Signal

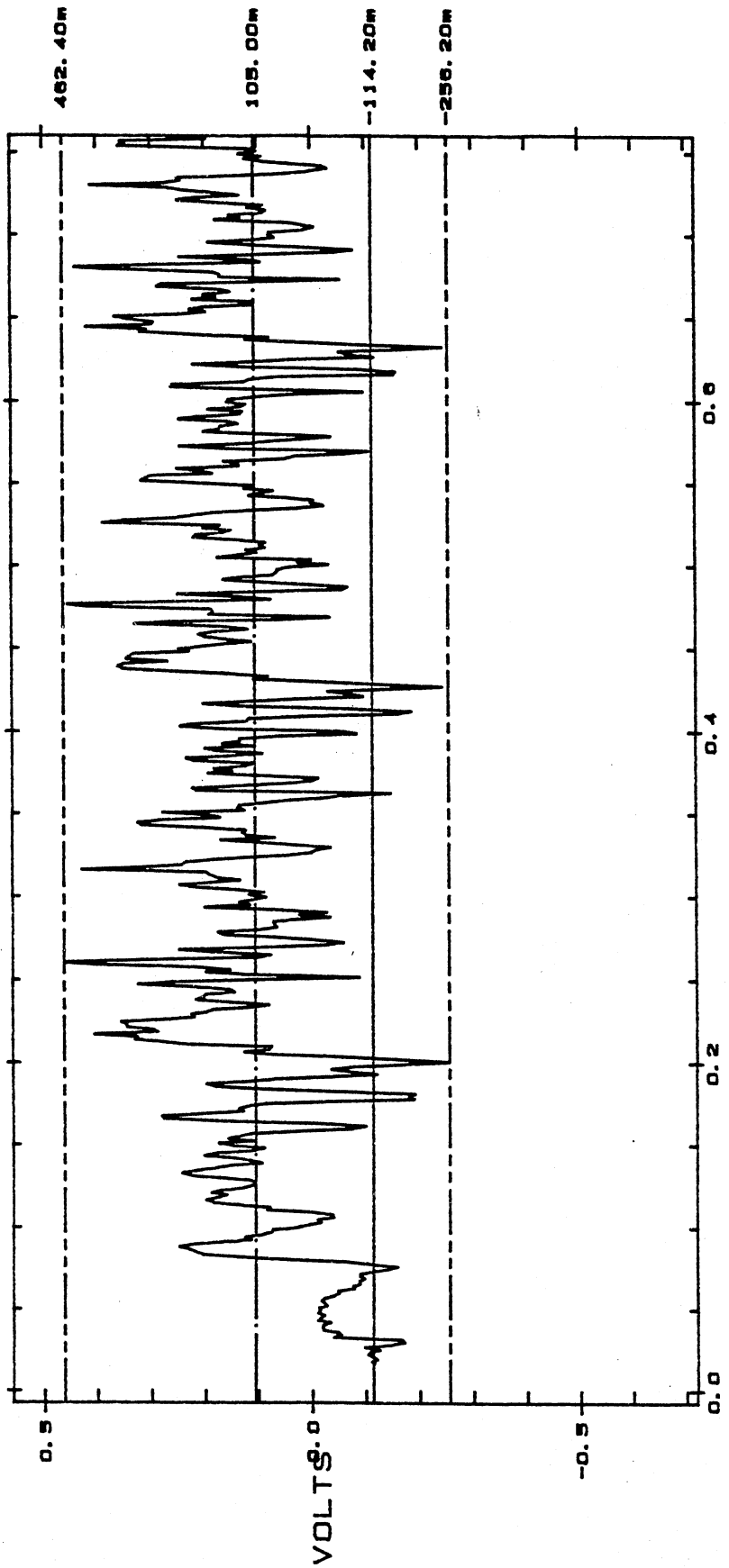

Figure 34. Production Head Response at Startup, Roll Signal

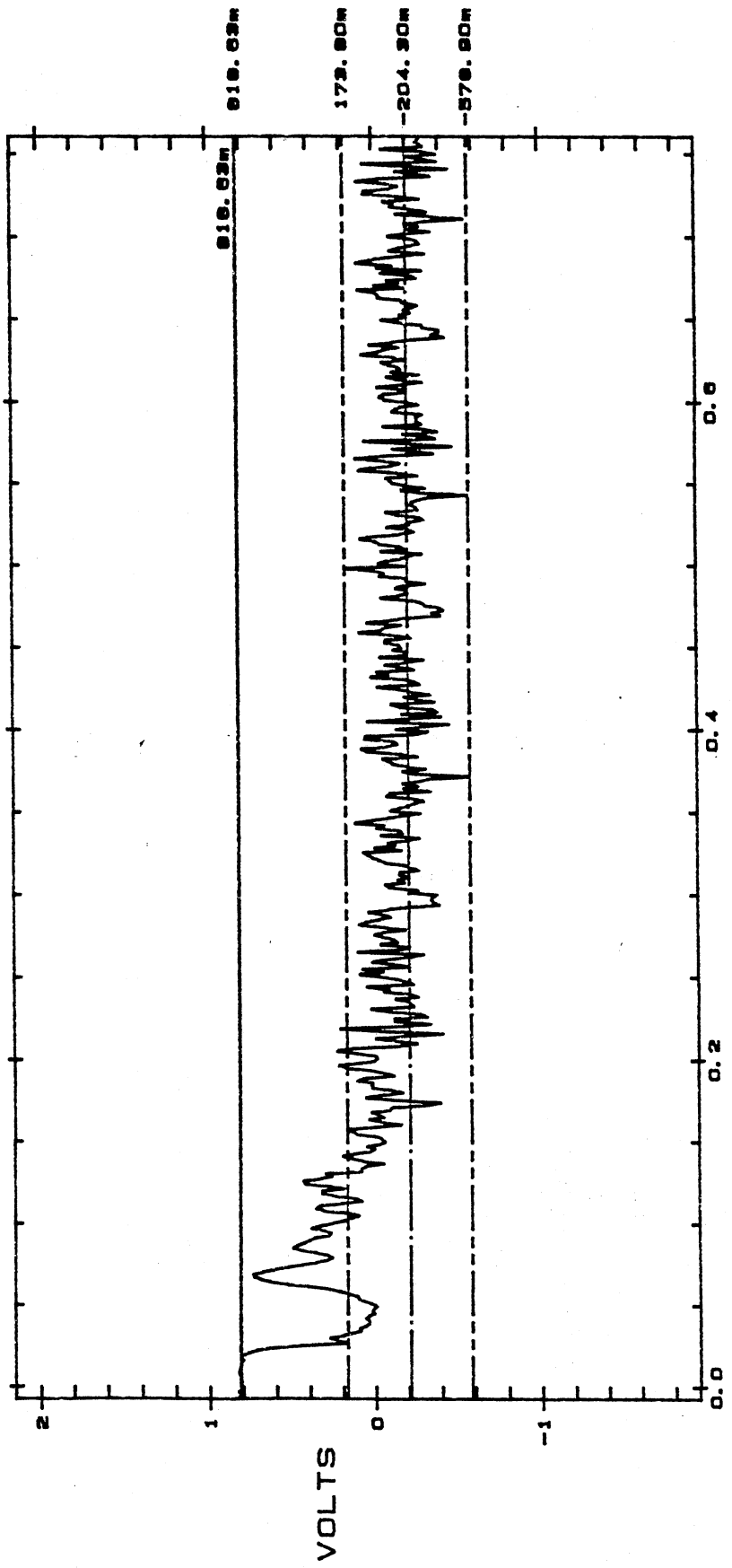

Figure 35. AD-4 Response at Startup, Pitch Signal

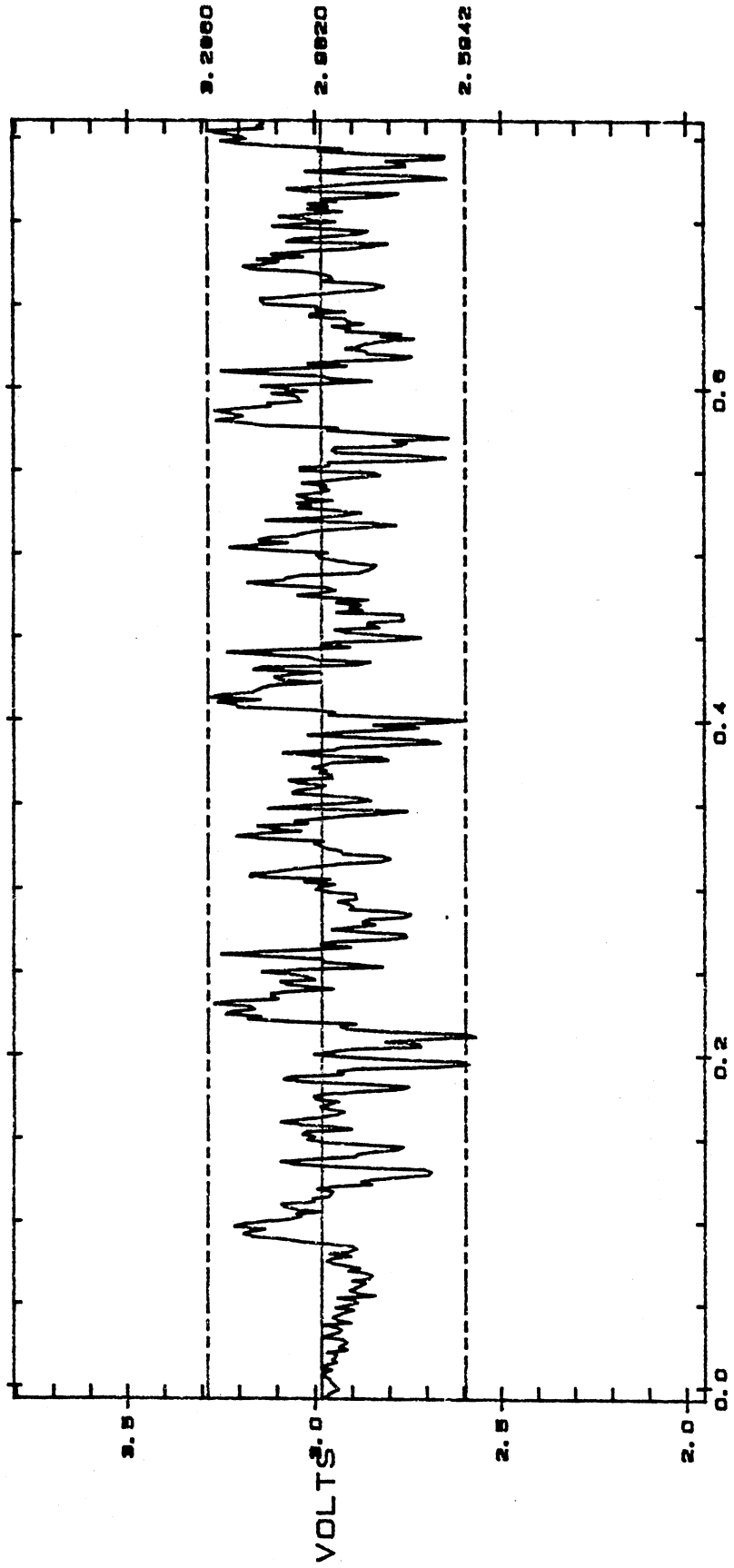

Figure 36. AD-4 Response at Startup, Roll Signal

TABLE XX

STEADY-STATE OFFSET AND MAXIMUM ROTATION AMPLITUDES
OF THE PRODUCTION HEAD AND AD-4

Maximum Displacement Amplitudes (°)	Production Head	AD-4
Pitch Rotation Offset	9.00(-3)	11.80(-3)
Roll Rotation Offset	3.40(-3)	1.14(-3)
Maximum Pitch Amplitude	4.46(-3)	4.34(-3)
Maximum Roll Amplitude	5.53(-3)	4.29(-3)

formation of a stationary wavefront in the flexible disk upstream of the leading edge of the stylus as shown in Figure 37. The analytical work of Greenburg [2] supports this theory.

Inspection of the roll offset data of Table XX indicates that the two styli roll in opposite directions--the production head toward the inside of the disk and AD-4 toward the outside of the disk; however, it should be noted that the steady-state offset in the roll direction of both heads is a fraction of that in the pitch direction. Inspection of the pitch values suggests that both the production head and AD-4 have steady-state offset and maximum amplitude values which are nearly identical. This is a favorable indication that the addition of the LD-400 damping material has little effect on the head/disk compliance.

Comparison of Overall Damping of the Production Head and AD-4

Figures 38 and 39 show the response of the production head and AD-4 after the drive motor has been shut off. Inspection of these figures indicates that the roll rotations of both styli cease immediately; however, both styli oscillate in the pitch direction as they attempt to return to their undeflected rest position. The production head oscillates at a frequency of 267 Hz. This frequency corresponds to the first pitch mode of the gimbal/stylus system as found in previous research. The frequency of oscillation evident in AD-4 is 286 Hz.

The decay rate of this vibration can be used to estimate the total head/disk system damping. The log decrement method was used to estimate an equivalent linear damping ratio. The equivalent linear damping ratio for the production head was found to be 0.04 and for AD-4 it was found

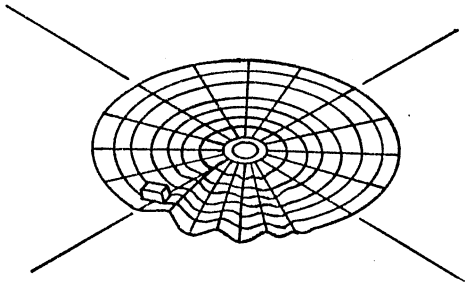

Figure 37. Stationary Wavefront Formed Upstream of Slider

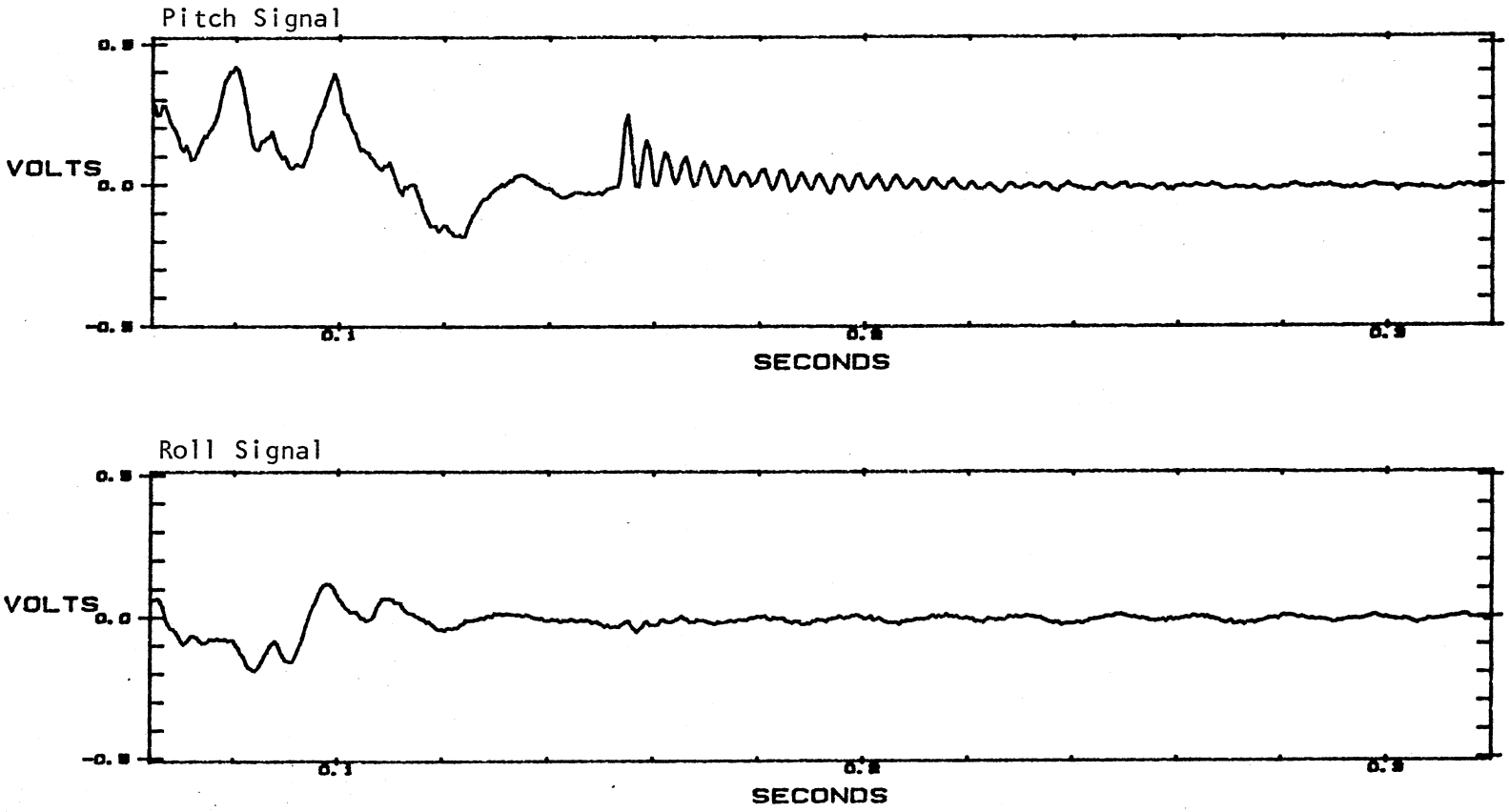

Figure 38. Production Head Response After Drive Shutoff

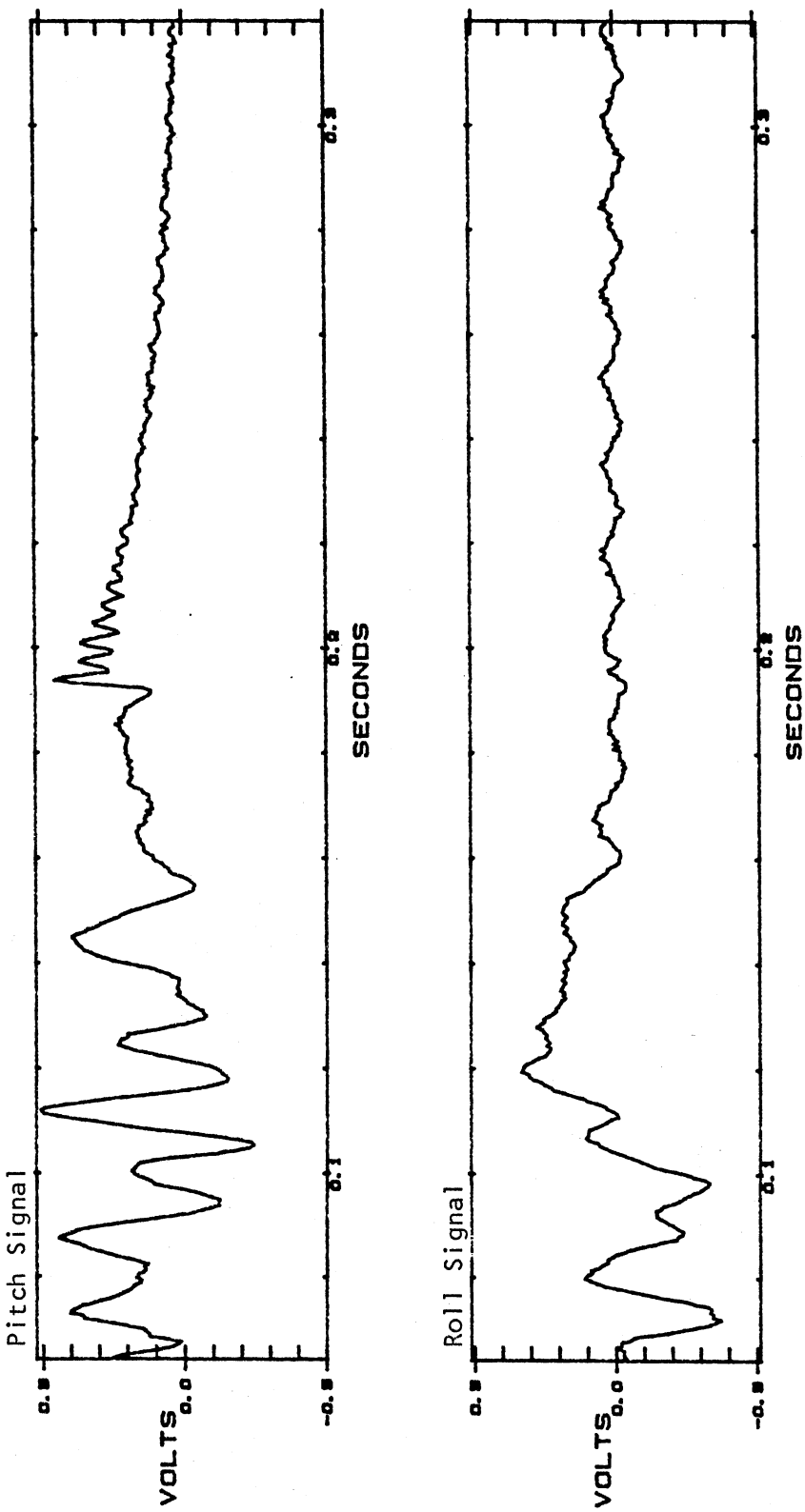

Figure 39. AD-4 Response After Drive Shutoff

to be 0.05. This indicates, as expected, that AD-4 has some amount of additional damping.

It is suspected that some portion of the calculated damping ratios is due to Coulomb-type frictional damping associated with relative motion between the head and disk. Relative vibration of this amplitude is not expected to occur during steady-state drive operation, as such amplitudes would likely cause read/write errors. Since a portion of the damping is associated with friction, the damping ratios that were calculated are not applicable to the high-frequency vibrations as it is the friction which induces these modes. For the purpose of this study, the damping ratios are to be used only to examine the additional damping effects, in AD-4, caused by the addition of the LD-400 damping material.

Correlation Between Pitch and Roll Signals of the Production Head

The A-RBA system was used in an attempt to determine if there are high-frequency vibration modes which occur in a direction which is a combination of both pitch and roll rotation directions. The DATA 6000 was used to cross-correlate the pitch and roll signals of one detector. A FFT was then performed on the resulting cross-correlation. The frequency spectrum (i.e., cross-spectral density) obtained through this process can then be inspected for frequency peaks which would indicate modes that could possibly be a combination of both pitch and roll.

Figure 40 contains the pitch spectrum, roll spectrum, and cross-spectrum that were acquired for this examination. A survey of the cross-spectrum indicates that there is much correlation between the pitch and roll signals at low frequencies. In the higher frequency range, there

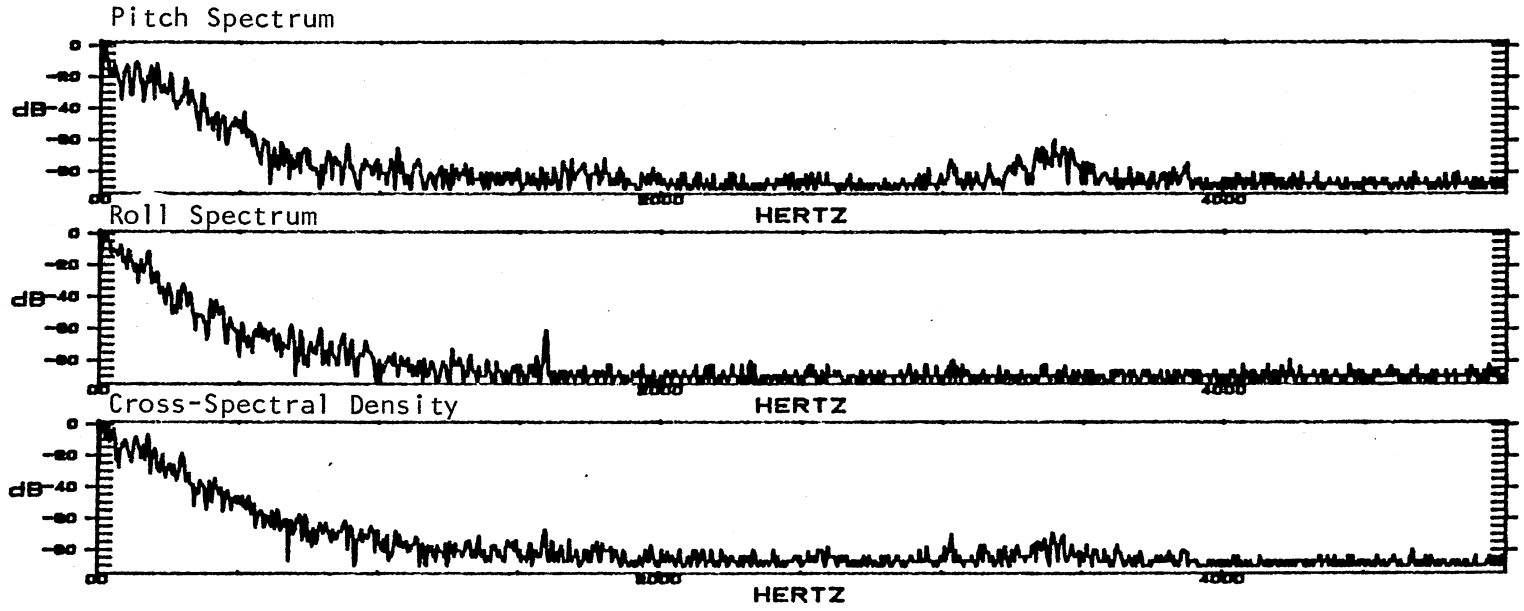

Figure 40. Spectra Representing Correlation Between Pitch and Roll Modes of the Production Head

appears to be only three frequency values which are possibly composed of both pitch and roll rotations. These frequencies are at 1592, 3037, and 3400 Hz. The 1592 Hz component is seen to be a dominant peak in the roll spectrum while it is not apparent in the pitch spectrum. This leads to the conclusion that the 1592 Hz peak in the cross-spectrum is only a showing of the dominance of this mode in the roll signal and it is not likely that this mode can be associated with pitch rotation. A similar deduction can be made for the 3400 Hz component in that it is a dominant mode in the pitch signal but is not seen to be present in the roll signal.

The 3037 Hz peak is apparent in both the pitch and roll spectra as well as in the cross-spectrum. This is a strong indication that this mode of vibration occurs in a direction which is a combination of pitch and roll. It should be pointed out that this mode is of no greater significance than the other high-frequency modes; it merely provides a better understanding of the movements associated with high-frequency vibration.

CHAPTER V

CONCLUSIONS

The objective of this study was to develop an instrument which could be used to analyze the dynamic motion of flexible disk drive read/write heads, in particular, the stylus of the read/write head. The systems that were developed proved to provide much information about the effects of head/disk interaction and the stylus motions which result from this interaction.

Conclusions Regarding Head/Disk Interaction and Stylus Motion

It was found that high-frequency vibration of the stylus was, overall, only a minor contributor to the total amplitude of the stylus motion. The data reveal that the low-frequency motion, which is the major motion component, is nearly periodic and is closely associated with waves in the flexible disk. The high-frequency vibrations of the stylus are excited by the frictional contact between the stylus and disk. This excitation is broad-band and is generally not seen to have measurable effects past 5 KHz.

The production head that was used in a major portion of the testing had a dominant high-frequency pitch motion in the 3600 Hz range. The high-frequency forcing function generated much excitation in the pitch direction, but the 3600 Hz component was by far the most significant

pitch mode. The bandwidth of the 3600 Hz peak can be viewed as an indication of the amount of damping present for that mode if the forcing function exhibits a near uniform amplitude at frequencies near (above and below) the peak value. The dominance of the 3600 Hz mode could indicate the broad-band excitation is at its greatest amplitude in this region; however, examination of the pitch spectra of designs AD-2 and AD-3 indicate that dominant high-frequency pitch modes can and do exist in other significantly different frequency ranges.

Other less significant pitch modes were seen to exist in the production head but were not evident consistently. The amplitude of the high-frequency modes were not truly consistent, but it was evident that vibrational amplitudes increase with increasing media velocities with all other factors being held constant.

The production head has a dominant roll mode at about 1600 Hz. The peak in the frequency spectrum associated with this frequency is more defined (narrower bandwidth) as compared with that of the 3600 Hz pitch mode. The narrow bandwidth of the 1600 Hz roll mode suggests that there is little damping associated with this mode. All of the heads that were tested (production head, AD-2, AD-3, and AD-4) exhibit a well defined roll mode in the 1600 to 1850 Hz region. It was also evident that these modes exhibit similar rotational amplitudes.

The experimental head designs that were constructed in attempts to reduce the amplitude of high-frequency vibrations proved, in part, to be a success. Designs AD-2 and AD-3 provided little reduction in high-frequency motions; however, design AD-4 effectively eliminated vibrations above 1000 Hz in the pitch direction and some reduction in the roll

amplitudes was evident also. The modifications made in design AD-4 had little effect on the low-frequency motions.

The A-RBA system was built in a quest to determine simultaneously the pitch, roll, and vertical translation of the stylus. Use of the A-RBA system indicated that, with the relative vibrational amplitudes associated with stylus motion, the system is much more sensitive (at least ten times more) to rotations as it is to translations. Being such, the translations that were calculated are not known to be accurate. It should be understood that the system sensitivity to rotations and translations is relative and must be analyzed for the particular motions that are to be examined. Using the maximum rotation amplitudes that were found (about 0.0045°) and assuming that the translation values have a magnitude on the order of 0.001 inches, the value of R would be required to be reduced by a factor of 10 (thus R would be about 3.5 inches) to make the system equally sensitive to the relative motion amplitudes. This would effectively reduce the rotation amplitude sensitivity by about 90 percent. A reduction of this magnitude would certainly reduce the system resolution, possibly to a degree which would render the system useless for examination of the low-amplitude high-frequency motions.

Although the A-RBA system was not totally effective in accurately determining translation values, it did allow for simultaneous analysis of pitch and roll rotations. This fact, in itself, made the A-RBA system worthy of the effort involved. The A-RBA system was useful in comparing pitch and roll signals of both low- and high-frequency.

Tests performed with the A-RBA system revealed that the leading edge of the stylus raises upward in the transition from rest to steady-state drive operation. This fact is true for both the production head and

AD-4, which were the only head designs tested with the A-RBA system. The styli also revealed a tendency to roll to one side or the other in steady-state operation. The production head rolled toward the inside radius and AD-4 rolled toward the outside radius. It should be noted that the offset in the roll direction is significantly smaller than the offset in the pitch direction for both head designs. The factor that determines which direction that the head rolls is not known in certainty. More intensive studies on a number of additional heads may show that the roll offset direction does not follow a set pattern.

An analysis of the cross-spectral density of the production head revealed that, of the dominant high-frequency modes, only a 3037 Hz component was seen to exist in the spectra of both pitch and roll signals. This technique did not prove to be of much use since a visual comparison of the pitch and roll spectra results in the same conclusions.

Conclusions Regarding RBA System

Accuracy and Resolution

The accuracy of the RBA systems is closely related to the calibration procedure and the assumptions made regarding restrained degrees of freedom. The detector sensitivities that were calculated in the calibration procedure are expected to be accurate in sensitivity magnitude within ±10 percent. This figure is merely an estimation, but calibration of the linear-lateral effect photodiode revealed that the three calibration procedures were in agreement within such bounds.

The degrees of freedom that are assumed to be restrained (yaw rotation and translation in x- and y-directions), in theory, will not effectively displace the reflected beam. There is undoubtedly some motion

associated with these components, but the RBA systems are very insensitive to such motions in comparison with the sensitivity to pitch, roll, and vertical translation.

The resolution of the RBA systems is governed by the system parameters R and ψ, the sensitivity of the detectors, and the resolution of the signal analysis equipment. Since the RBA systems are used to examine pitch rotations and roll rotations as well as vertical translations, the resolution must be considered for each motion component.

Considering the above mentioned parameters, it is estimated that the following resolutions apply for the RBA systems:

Resolution for rotations: 2.0(-6) degrees

Resolution for translations: 7.0(-6) inches

Note that this does not necessarily imply expected accuracy. As a final comment, the RBA systems are limited to examination of frequencies of less than 5 KHz by the 301-DIV amplifiers; however, amplifiers with a flat frequency response up to 30 KHz are available.

Recommended RBA System Refinements

The RBA systems proved to be very useful and reasonably accurate; however, the author believes that the following system refinements will allow for greater system accuracy and certainty:

1. A more powerful laser is needed for the A-RBA system, as the beam intensity of the present laser (0.95 mW) is marginal for proper use of the array detectors. Also, a beam diameter of about 0.2 mm would be more suitable for use in the system due to the small size of the mirror that is mounted on the stylus.

2. Examine the results of using reduced values of R so that the relative system sensitivity to rotation and translation is more balanced.

3. A precise calibration procedure that will allow for examination of high-frequency system responses is needed. One calibration system which might prove to be suitable is a piezoelectric system such as the method discussed by Pinder and Palmer [11].

REFERENCES

[1] Engh, J. T. "The IBM Diskette and Diskette Drive." IBM Journal of Research and Development, Vol. 25 (1981), pp. 701-710.

[2] Greenberg, H. J. "Flexible Disk-Read/Write Head Interface." IEEE Transactions on Magnetics, Vol. 14 (1978), pp. 336-338.

[3] Charbonnier, P. P. "Flight of Flexible Disk Over Recording Heads." IEEE Transactions on Magnetics, Vol. 12 (1976), pp. 728-730.

[4] Smith, P., and H. Ragle. "High Speed Flexible Disk-Head Interface." IEEE Transactions on Magnetics, Vol. 15 (1979), pp. 1459-1461.

[5] Lin, C. "Techniques for the Measurement of Air-Bearing Separation --A Review." IEEE Transactions on Magnetics, Vol. 9 (1973), pp. 673-677.

[6] Chiou, A. E. "The Effect of Spring Pad Loading and Head Penetration on the Flight of Flexible Disk Over a Spherical Head." IEEE Transactions on Magnetics, Vol. 21 (1985), pp. 20-27.

[7] Good, James K. "The Development of Finite Element Modeling and Experimental Techniques for Dynamic Analysis of Read/Write Head Designs on Floppy Disk Media." (Unpub. Ph.D. dissertation, Oklahoma State University, 1983.)

[8] Vickery, C. M., J. K. Good, and R. L. Lowery. "Experimental Analysis of Displacements of Read/Write Heads Upon Floppy-Disk Media." Experimental Mechanics, Vol. 25 (1985), pp. 200-203.

[9] Swedeen, Randall J. "Vibration Analysis of a Floppy Disk Head." (Unpub. M.S. report, School of Mechanical and Aerospace Engineering, Oklahoma State University, 1982.)

[10] Bouchard, G., D. B. Bogy, and F. E. Talke. "An Experimental Comparison of the Head/Disk Interface Dynamics in 5¼- and 8-Inch Disk Drives." IBM Journal of Research and Development, Vol. 29 (1985), pp. 316-322.

[11] Pinder, A. C., and A. R. Palmer. "A Novel Technique for Measuring Small Vibrations." Journal of Physics E, Vol. 15 (1982), pp. 478-484.

[12] Cook, R. O., and C. W. Hamm. "Fiber Optic Lever Displacement Transducer." Applied Optics, Vol. 18 (1979), pp. 3230-3241.

[13] Ueha, S., N. Shibata, and J. Tsujuichi. "Flexible Coherent Optical Probe for Vibration Measurement." Optics Communications, Vol. 23 (1977), pp. 407-409.

[14] Garza, R., and B. Sharp. "A Review of Holographic Techniques for Structural Analysis." Sound and Vibration, Vol. 19 (1985), pp. 28-30.

[15] Kelly, B. O. "Lateral-Effect Photodiodes." Laser Focus, Vol. 11 (1976), pp. 38-40.

[16] Gerald, Curtis F., and P. O. Wheatly. Applied Numerical Analysis. 3rd ed. Reading, Mass.: Addison-Wesley, 1984.

[17] Hanson, W. J., and G. A. Hampel. "A Performance Comparison of Vibration Damping Materials." Sound and Vibration, Vol. 18 (1984), pp. 22-35.

[18] Doebelin, Ernest O. Measurement Systems Application and Design. 3rd ed. New York: McGraw-Hill, 1983.

APPENDIX

```
C-------------------------------------------------------------
C     FLOPPY DISK VIBRATION STUDY
C     FOUR CHANNEL SYSTEM DATA REDUCTION PROGRAM
C
C     PROGRAM READS VOLTAGE DATA TAKEN FROM THE FOUR
C     CHANNEL SYSTEM AND CALCULATES THE PITCH, ROLL,
C     AND VERTICAL TRANSLATION OF THE READ/WRITE HEAD.
C     ACCURACY CALCULATIONS ARE PERFORMED ON THE ROLL
C     DISPLACEMENT; HOWEVER, NO ERROR CALCULATION
C     CAN BE ESTIMATED FOR THE PITCH OR TRANSLATION SINCE
C     THERE IS NO ALTERNATE SIGNAL FOR COMPARISON.
C
C     INPUT DATA SET:
C       DSET - PROGRAM PROMPTS FOR NAME OF INPUT
C              DATA SET AND ASSIGNS THIS NAME TO
C              THE CHARACTER VARIABLE DSET
C
C     DATA INPUT PARAMETER
C       INVOLT - SPECIFIES WHETHER INPUT VOLTAGES ARE
C                AC OR DC:
C                         INVOLT = 0 >>>>> INPUT IS AC
C                         INVOLT = 1 >>>>> INPUT IS DC
C                ****************************************
C                ** IF INPUT IS DC, THE PROGRAM ASSUMES **
C                ** THAT THE FIRST LINE OF DATA READ IS **
C                ** THE ZERO REFERENCE FOR ALL DATA     **
C                ****************************************
C
C     INPUT VARIABLES:
C       TIME - DATA POINT REFERENCE TIME IN mSx1E3
C       PT1  - VOLTAGE OF PITCH AND TRANSLATION SIGNAL
C              FROM DETECTOR ONE (UPPER) IN mVx1E3
C       PT2  - VOLTAGE OF PITCH AND TRANSLATION SIGNAL
C              FROM DETECTOR TWO (LOWER)IN mVx1E3
C       RR1  - VOLTAGE OF ROLL SIGNAL FROM DETECTOR ONE
C              IN mVx1E3
C       RR2  - VOLTAGE OF ROLL SIGNAL FROM DETECTOR TWO
C              IN mVx1E3
C
C     VARIABLES USED IN MAIN PROGRAM
C       NPTS   - NUMBER OF DATA SETS READ FROM INPUT
C       SENS   - SENSITIVITY OF DETECTORS IN V/IN
C       OA     - DISTANCE FROM MIRROR TO DETECTOR
C                SURFACE IN INCHES
C       PSI    - 90.0 DEG MINUS ANGLE FROM MIRROR NORMAL
C                TO CENTER LINE OF THE LOWER DETECTOR
C       PI     - ACCURATE REPRESENTATION OF PI
C       PITCH1 - PITCH ANGLE CALCULATED FROM DETECTOR ONE
C       PITCH2 - PITCH ANGLE CALCULATED FROM DETECTOR TWO
C       ROLL1  - ROLL ANGLE CALCULATED FROM DETECTOR ONE
C       ROLL2  - ROLL ANGLE CALCULATED FROM DETECTOR TWO
C       TRANS  - VERTICAL TRANSLATION CALCULATED FROM
C                THE DIFFERENCE IN PT1 AND PT2
```

```
C       RACCUR - ACCURACY EXPRESSED AS THE DIFFERENCE
C                BETWEEN ROLL1 AND ROLL2
C       PMAX   - MAXIMUM PITCH ANGLE
C       RMAX   - MAXIMUM ROLL ANGLE
C       TRMAX  - MAXIMUM VERTICAL TRANSLATION
C       IP     - INDEX CORRESPONDING TO MAX PITCH
C       IR     - INDEX CORRESPONDING TO MAX ROLL
C       ITR    - INDEX CORRESPONDING TO MAX TRANSLATION
C
C     OUTPUT FILES
C       PITCH - OUTPUT OF CALCULATED PITCH ANGLES
C       ROLL  - OUTPUT OF CALCULATED ROLL ANGLES
C       VTRAN - OUTPUT OF CALCULATED VERTICAL TRANSLATIONS
C
C-----------------------------------------------------------------
      REAL PITCH1(70),PITCH2(70),ROLL1(70),ROLL2(70),RACCUR(70)
     $,DIFF(70),TRANS(70),PT1(70),PT2(70),RR1(70),RR2(70),TIME(70)
      CHARACTER*17 DSET
      SENS=71.0
      OA=35.0
      PSI=48.5
      PI=4.0*ATAN(1.0)
      PMAX=0.0
      RMAX=0.0
      TRMAX=0.0
      WRITE(3,*)'ENTER NAME OF INPUT DATA SET'
      READ(3,50)DSET
   50 FORMAT(A17)
      WRITE(3,*)'ARE THE INPUT VOLTAGES      0) -- AC'
      WRITE(3,*)'                          OR 1) -- DC'
      READ(3,*)INVOLT
      OPEN(UNIT=4,FILE=DSET)
      NPTS=0
C
C     READ VOLTAGES FROM DSET
C
      DO 100 JJ=1,70
        READ(4,*,END=150)TIME(JJ),PT1(JJ),PT2(JJ),RR1(JJ),RR2(JJ)
        WRITE(3,*)JJ,TIME(JJ),PT1(JJ),PT2(JJ),RR1(JJ),RR2(JJ)
        PT1(JJ)=PT1(JJ)*1E-3
        PT2(JJ)=PT2(JJ)*1E-3
        RR1(JJ)=RR1(JJ)*1E-3
        RR2(JJ)=RR2(JJ)*1E-3
        NPTS=NPTS+1
  100 CONTINUE
  150 CLOSE(UNIT=4)
C
C     SCALE INPUTS IF THEY ARE DC
      IF(INVOLT.EQ.1)THEN
        DO 180 JJ=2,NPTS
          PT1(JJ)=PT1(JJ)-PT1(1)
          PT2(JJ)=PT2(JJ)-PT2(1)
          RR1(JJ)=RR1(JJ)-RR1(1)
          RR2(JJ)=RR2(JJ)-RR2(1)
```

```
  180   CONTINUE
        PT1(1)=0.0
        PT2(1)=0.0
        RR1(1)=0.0
        RR2(1)=0.0
      END IF
C
C     CALCULATE DISPLACEMENTS (TRANSLATION,PITCH, AND ROLL)
C
      DO 200 JJ=1,NPTS
C     CALCULATE VERTICAL TRANSLATION
C
      DIFF(JJ)=PT2(JJ)-PT1(JJ)
      TRANS(JJ)=DIFF(JJ)/(2.0*SENS)
      TRANS(JJ)=TRANS(JJ)/(COS(PSI*PI/180.0)-COS((PSI+20.0)*PI/180.0))
      IF(ABS(TRANS(JJ)).GT.ABS(TRMAX))ITR=JJ
      IF(ABS(TRANS(JJ)).GT.ABS(TRMAX))TRMAX=TRANS(JJ)
C
C      CALCULATE PITCH ROTATIONS
C
       PITCH1(JJ)=PT1(JJ)-2.0*TRANS(JJ)*SENS*COS((PSI+20.0)*PI/180.0)
       PITCH2(JJ)=PT2(JJ)-2.0*TRANS(JJ)*SENS*COS(PSI*PI/180.0)
       PITCH1(JJ)=PITCH1(JJ)/(2.0*OA*SENS)*180.0/PI
       PITCH2(JJ)=PITCH2(JJ)/(2.0*OA*SENS)*180.0/PI
       IF(ABS(PITCH1(JJ)).GT.ABS(PMAX))IP=JJ
       IF(ABS(PITCH1(JJ)).GT.ABS(PMAX))PMAX=PITCH1(JJ)
C
C      CALCULATE ROLL ROTATIONS
C
       ROLL1(JJ)=RR1(JJ)/(2.0*SENS*OA*SIN((PSI+20.0)*PI/180.0))
     $*180.0/PI
       ROLL2(JJ)=RR2(JJ)/(2.0*SENS*OA*SIN(PSI*PI/180.0))
     $*180.0/PI
       IF(ABS(ROLL1(JJ)).GT.ABS(RMAX))IR=JJ
       IF(ABS(ROLL1(JJ)).GT.ABS(RMAX))RMAX=ROLL1(JJ)
       IF(ABS(ROLL2(JJ)).GT.ABS(RMAX))IR=JJ
       IF(ABS(ROLL2(JJ)).GT.ABS(RMAX))RMAX=ROLL2(JJ)
       RACCUR(JJ)=(ROLL1(JJ)-ROLL2(JJ))
  200 CONTINUE
C
C      OUTPUT TO FILES PITCH, ROLL, AND VTRAN
C
       OPEN(UNIT=7,FILE='          PITCH')
       WRITE(7,*)'****PITCH DATA****'
       WRITE(7,*)
       WRITE(7,*)' TIME         PITCH     '
       WRITE(7,*)' (mS)         (DEG)     '
       WRITE(7,*)'----------------------'
       DO 300 JJ=1,NPTS
         WRITE(7,250)TIME(JJ),PITCH1(JJ)
  250    FORMAT(1X,F6.1,4X,G10.4)
  300  CONTINUE
       WRITE(7,*)'----------------------'
       WRITE(7,*)'MAXIMUM PITCH ANGLE'
```

```
      WRITE(7,250)TIME(IP),PITCH1(IP)
      CLOSE(UNIT=7)
      OPEN(UNIT=8,FILE='            ROLL')
      WRITE(8,*)'****ROLL DATA****'
      WRITE(8,*)
      WRITE(8,*)' TIME        ROLL1          ROLL2        ACCURACY'
      WRITE(8,*)' (mS)        (DEG)          (DEG)         (DEG) '
      WRITE(8,*)'-------------------------------------------------'
      DO 400 JJ=1,NPTS
        WRITE(8,350)TIME(JJ),ROLL1(JJ),ROLL2(JJ),RACCUR(JJ)
350     FORMAT(1X,F6.1,4X,3(G10.4,4X))
400   CONTINUE
      WRITE(8,*)'-------------------------------------------------'
      WRITE(8,*)'MAXIMUM ROLL ANGLE'
      WRITE(8,350)TIME(IR),ROLL1(IR),ROLL2(IR),RACCUR(IR)
      CLOSE(UNIT=8)
      OPEN(UNIT=9,FILE='           VTRAN')
      WRITE(9,*)'****TRANSLATION DATA****'
      WRITE(9,*)
      WRITE(9,*)' TIME       TRANSLATION'
      WRITE(9,*)' (mS)        (INCHES)    '
      WRITE(9,*)'-----------------------'
      DO 500 JJ=1,NPTS
        WRITE(9,450)TIME(JJ),TRANS(JJ)
450     FORMAT(1X,F6.1,6X,G10.4)
500   CONTINUE
      WRITE(9,*)'-----------------------'
      WRITE(9,*)'MAXIMUM TRANSLATION'
      WRITE(9,450)TIME(ITR),TRANS(ITR)
      CLOSE(UNIT=9)
      STOP
      END
```

VITA

Dennis Lynn Miller

Candidate for the Degree of

Master of Science

Thesis: AN EXPERIMENTAL TECHNIQUE FOR DYNAMIC ANALYSIS OF FLEXIBLE DISK DRIVE READ/WRITE HEAD DESIGNS

Major Field: Mechanical Engineering

Biographical:

Personal Data: Born in Springdale, Arkansas, April 28, 1962, the son of Mr. and Mrs. Chester W. Miller.

Education: Graduated from Springdale High School, Springdale, Arkansas, in May, 1980; received the Bachelor of Science in Mechanical Engineering degree from Oklahoma State University in 1984; completed requirements for the Master of Science degree at Oklahoma State University in December, 1985.

Professional Experience: Project Engineer, Sun Refining and Marketing Co., Tulsa, Oklahoma, 1983; Teaching and Research Assistant, School of Mechanical and Aerospace Engineering, Oklahoma State University, 1984-1985.

Professional Organizations: Tau Beta Pi, Pi Tau Sigma, American Society of Mechanical Engineers, Oklahoma Society of Professional Engineers.